Advances in the Quantum Theoretical Approach to Image Processing Applications

NOUR ABURA'ED, Visual Signal Analysis and Processing (VSAP) Research Center, Khalifa University of Science, Technology, and Research, Abu Dhabi, UAE
FAISAL SHAH KHAN, Quantum Computing Research Group, Department of Applied Math and Science, Khalifa University of Science, Technology, and Research, Abu Dhabi, UAE
HARISH BHASKAR, Visual Signal Analysis and Processing (VSAP) Research Center, Khalifa University of Science, Technology, and Research, Abu Dhabi, UAE

In this article, a detailed survey of the quantum approach to image processing is presented. Recently, it has been established that existing quantum algorithms are applicable to image processing tasks allowing quantum informational models of classical image processing. However, efforts continue in identifying the diversity of its applicability in various image processing domains. Here, in addition to reviewing some of the critical image processing applications that quantum mechanics have targeted, such as denoising, edge detection, image storage, retrieval, and compression, this study will also highlight the complexities in transitioning from the classical to the quantum domain. This article shall establish theoretical fundamentals, analyze performance and evaluation, draw key statistical evidence to support claims, and provide recommendations based on published literature mostly during the period from 2010 to 2015.

CCS Concepts: • **Theory of computation** → **Quantum information theory**; • **Computing methodologies** → **Image processing**; • **Hardware** → **Quantum computation**; • **Security and privacy** → *Information-theoretic techniques*; • **Computing methodologies** → *Computer vision*

Additional Key Words and Phrases: Quantum computing, image processing, image denoising, edge detection, image storage, image retrieval, image compression, image watermarking

ACM Reference Format:
Nour Abura'ed, Faisal Shah Khan, and Harish Bhaskar. 2016. Advances in the quantum theoretical approach to image processing applications. ACM Comput. Surv. 49, 4, Article 75 (February 2017), 49 pages.
DOI: http://dx.doi.org/10.1145/3009965

1. INTRODUCTION

The origins of quantum physics trace back to a scientific work by Planck [1900] in which the paradox of ultraviolet catastrophe was resolved. Ultraviolet catastrophe was an idea based on the principles of the prevailing "classical" physics of the time—that an object at thermal equilibrium will emit radiation at all frequencies and emit more energy at higher frequencies. This led to the conclusion that the total amount of energy emitted by such an object would be infinite, contradicting not only the law of conservation of energy but also experimental observations. Planck's solution to this paradox was to postulate that energy could only come in discrete packets or *quanta*.

Authors' addresses: N. Abura'ed and H. Bhaskar, Visual Signal Analysis and Processing (VSAP) Research Center, Dept. of Electrical and Computer Engineering, Khalifa University, P.O. Box: 127788, Abu Dhabi, UAE; emails: {nour.aburaed, harish.bhaskar}@kustar.ac.ae; F. S. Khan, Quantum Computing Research Group, Department of Applied Mathematics and Sciences, Khalifa University, P.O. Box: 127788, Abu Dhabi, UAE; email: faisal.khan@kustar.ac.ae.

DOI: http://dx.doi.org/10.1145/3009965

This assumption led to the conclusion that the average energy released from the object would decrease with the frequency, so as frequency goes to infinity, the average energy goes to zero, preserving the conservation of energy law and reconciling experimental observations. A thorough review of the history of the derivation of Planck's formula that gave birth to quantum physics can be found in Boya [2004].

Toward the 20th century, quantum physics further developed and cemented its position as the "new" physics governing the dynamics of the atomic and subatomic world. In 1905, Einstein [1965] successfully explained the photoelectric effect, where light incident on an object leads to the emission of electrons from the object's atoms. The success of Einstein's explanation was based on an assumption that light was made up of quanta, or photons, rather than waves, an idea motivated by Planck's seminal work mentioned earlier. This work earned Einstein the Nobel Prize in physics in 1921. Furthermore, in 1913, Bohr proposed a model of the hydrogen atom by assuming discrete or quantum values for angular momentum of the electron [Bohr 1913]. This model explained experimentally observed properties of the hydrogen atom that other prevailing models of the time could not. Further developments in formalizing the physics of the quanta by Born [1926], Dirac [1930], Heisenberg [1927], and Schrödinger [1926] culminated in a formal theory of quantum physics. This theory, sometimes referred to as the old quantum theory, has been responsible for the ensuing decades of major technological innovations such as the transistor (and hence computers) and the laser (and hence CD-ROMs, Blu-ray, etc). An excellent treatment of the ubiquity of the old quantum theory can be found in Kakalios [2011].

Since the late 1980s, quantum physics has once again come to the forefront of technological innovation in a dramatic way. In fact, it would be appropriate to say that a "new quantum theory" has come to light in the past four decades, which sees the old quantum theory fuse together with the theory of information processing. At least one each of scientific philosophies and technological advances have led to this fusion of information and quantum physics, with the former being Richard Feynman's idea that a computational perspective on quantum physics might produce an efficient method to simulate complex quantum physical systems like molecules. This idea was further developed by Deutsch [1985]. The fact that the number of processors on a computer chip has been roughly doubling every year since the 1980s had a major role in the development of what is now known as quantum information processing. This trend in computer engineering, referred to as Moore's law [Moore 1965], means that the physical size of these processors has been decreasing rapidly and by 2020 or so would reach the atomic scale. In this scenario, quantum effects, which were regarded as negligible noise in the technological innovations based on the old quantum theory would now have to be dealt with.

Motivated by developments such as Feynman's idea and Moore's law, scientists have studied the theoretical underpinnings of quantum computers, which are essentially Turing machines that utilize the principles of quantum mechanics, and which are expected to give dramatic computational speedups over the classical Turing machines. For example, the algorithms of Shor and Grover [Shor 1997; Grover 1996] are designed to run on a quantum computer in durations that are polynomial and quadratic in input size, respectively, for factoring integers and searching unstructured databases. Because the problems of integer factorization is known to be an NP problem on classical computers, it is extensively used in electronic security protocols such as the RSA and elliptic curve–based cryptography. The fact that a quantum computer can run Shor's algorithm in time that is polynomial in the size of the input means that these security protocols will become obsolete once a fully functioning quantum computer becomes available. In addition, since the complexity of the brute-force search of an unstructured database of k elements is $O(k)$, Grover's search algorithm offers a substantial speedup in this case. This observation got the attention of security experts and intelligence

communities worldwide and led to a flurry of interest from both academia and industrial stakeholders in quantum computer science. The culmination of this interest was the announcement in 2007 that D-wave, a Canadian technology company, had developed a commercially available quantum computer, albeit the fact that this first-generation quantum computer is analogous to the room-size ENIAC computer of the 1940s. However, it is not a general-purpose quantum computer. Rather, it is a quantum annealer that was developed to solve optimization problems. Nonetheless, this quantum machine was acquired by Lockheed Martin in 2011 and then by a consortium of Google and NASA in 2013. The goal of the latter acquisition is to use the D-wave quantum machine as a launch pad of an indigenous effort by Google scientists to create a quantum computer but with significantly advanced features than those of the D-wave machine, such as multifunctionality. Even though quantum computers and their first-generation realizations have shown promising results, it is important to note that in some cases, quantum algorithms are not superior in performance to their classical counterparts. An example of such cases is mentioned in Fijany and Williams [1998].

Quantum computational models for several information-theoretic constructs, such as image processing and big data analysis [Mastriani 2014a], have shown promise of enhanced results in computational efficiency. Big data refers to extremely large datasets that could be analyzed to reveal certain patterns or draw conclusions and associations. This takes an extensive amount of calculations since the size of data is significantly large. Big data clustering and classification algorithms have been proposed to run on quantum computers as well as for topological data analysis [Lloyd et al. 2016]. In case of the latter, the quantum algorithm for identifying the topological shape of the data performs dramatically faster than the corresponding classical algorithms. For instance, if there exists a space with n points and k scales, performing the classical persistent homology takes as much time as $O(2^{2n})$. On the other hand, the quantum algorithm takes as much time as $O(n^5)$ [Lloyd et al. 2016].

Images are one form that big data can take. Image processing has been studied extensively on classical computers beginning from image acquisition to image analysis dealing with enhancement, segmentation, transformations, and security. The use of quantum computation within the context of visual signal processing can potentially allow the handling of millions of visual signals simultaneously using the quantum mechanical principle of superposition (discussed in more detail in Section 2), without compromise in the computational demand [Dubey et al. 2014]. In particular, quantum models of image processing through modifications to existing classical techniques can dramatically improve the results of several image processing tasks in terms of speed and performance [Dubey et al. 2014], independent of the image size. Despite such overwhelming attention to quantum image processing (QuIP) in the recent years, one main challenge that remains is finding quantum algorithms that characterize images better and faster than their classical counterparts [Mastriani 2014a]. However, the first steps taken toward exploring the possibility of manipulating image pixels as quantum states have made the field of QuIP quite promising. This has primarily involved major improvements in hardware, such as the development and use of quantum computers [Beach et al. 2003]; however, without the development of compatible software techniques, accomplishing real-world use could become a daunting task.

Some initial research has been conducted in quantum image storage, retrieval, and compression [Li et al. 2013a, 2014; Venegas-Andraca and Ball 2010; Zhang et al. 2013c; Vlasov 1997; Beach et al. 2003; Venegas-Andraca 2003a, 2003b; Latorre 2005; Le et al. 2010; Yan et al. 2015a; Iliyasu et al. 2011]. Most of the researchers have approached these areas by exploiting the principles of quantum superposition and quantum entanglement that will be discussed in Section 2. Briefly, quantum superpositions are joint states of many quantum systems. Mathematically, the Cartesian product is the "standard" way to create a composite system from given individual systems. However,

other products, such as the tensor product, are also possible. In quantum physics, the tensor product is a more general construction allowing for the production of joint states that are correlated more strongly than states in any classical physical system. These latter joint quantum states are said to be entangled and are the source of enhanced results observed in quantum information processing. Baez [2004] provides an excellent discussion on the way the tensor product makes quantum physics dramatically different from classical physics.

There are also other lines of research that involve denoising [Pan et al. 2012; Brida et al. 2010; Mastriani 2014a; Bhattacharyya et al. 2014; Yuan et al. 2013; Wang and Li 2007; Zhou et al. 2010; Fu et al. 2010] and edge detection [Zhang et al. 2012; Dubey et al. 2014; Yi et al. 2014], in addition to preliminary research that has been accomplished in pseudocoloring, which is a branch of image enhancement [Jiang et al. 2015]. Some of these explorations mainly aim to extend the classical, well-known techniques into the quantum domain—for example, the median filter [Yuan et al. 2013; Zhou et al. 2010]. The main feature common to both noise and the quantum representation of bits is that both of them are probabilistic in nature—that is, both the quantum measurement of qubits (explained further in Section 2) and noise intensity can be modeled as a probability distribution. Hence, the filters that have been extended to the quantum domain appear more adaptive to the noise intensity because a pixel can have different possible states depending on the noise intensity (see Section 4 for more details). In addition, there have been initial studies conducted in image watermarking [Zhang et al. 2013b; Yang et al. 2013a; Song et al. 2013; Yang et al. 2014; Song et al. 2014a; Soliman et al. 2015; Iliyasu et al. 2012; Iliyasu 2013] that aim to enhance image security without distorting it or degrading its quality. Furthermore, preliminary research has been conducted for image understanding and transformations on quantum computers [Le et al. 2010, 2011c; Wang et al. 2015a; Jiang and Wang 2015; Yan et al. 2012a; Yan et al. 2012b; Zhou and Sun 2015; Yuan et al. 2014a; Zhou et al. 2015b; Caraiman and Manta 2009].

This article sheds light on some of the important QuIP techniques and their relevant applications. We also compare these quantum formulations to their classical counterparts using performance metrics such as the signal-to-noise ratio (SNR), peak signal-to-noise ratio (PSNR), and mean squared error (MSE). Some of the main novelty and contributions of this survey include:

—Detailed insights into the applications of quantum computing to image processing.
—Qualitative and quantitative comparison of existing QuIP techniques and their classical counterparts.
—A critical review of the advances and trends in image processing.
—A statistical summary of the studied techniques to draw recommendations for future work in this area.

The remainder of the article is organized as follows. A brief introduction to quantum information and computation is provided in Section 2. Further, the survey will review image processing techniques and their respective quantum equivalent techniques for image storage, retrieval, and compression in Section 3; image enhancement through denoising in Section 4; edge detection in Section 5; image understanding and computer vision in Section 6; image transformations in Section 7; and image security using digital watermarking, encryption, and scrambling in Section 8. Recommendations and possible future work for QuIP will be presented along with indicative quantitative results and a statistical summary of the literature in Section 9. We conclude in Section 10.

2. FUNDAMENTALS OF QUANTUM INFORMATION AND COMPUTING

Advances in computation technology over the past two decades have roughly followed Moore's law, which asserts that the number of transistors on a microprocessor doubles approximately every 2 years [Moore 1965]. Extrapolating this trend, somewhere

between the years 2020 and 2030, the circuits on a microprocessor will measure on an atomic scale. At this scale, quantum mechanical effects will materialize, and microprocessor design and engineering would have to account for these effects.

To this end, quantum information theory studies information processing under a quantum mechanical model. One goal of the theory is the development of quantum computers with the potential to harness quantum mechanical effects for enhanced computational capability [Khan 2009]. In addition, attention will have to be paid to quantum mechanical effects that may obstruct coherent computation.

Here, the fundamentals of quantum computing required for understanding the underlying principles of QuIP are introduced. Quantum mechanics offers flexibility to accommodate the growing computational needs and provides a unique perspective in explaining the behavior of conventional algorithms when these are implemented on an atomic scale. This point of view is important because as technology advances, the demand for high processing power and exponential storage capacity increases. As stated before, quantum computers utilize quantum physical effects to run quantum algorithms that are expected to outperform corresponding classical algorithms running on classical computers. The fundamentals of quantum physics responsible for this superior performance are discussed in the following sections.

2.1. Qubits and Quantum Superposition

The simplest quantum system is the qubit, which represents the general states of a quantum physical object, such as the photon or the electron. Mathematically, a qubit is an element of a two-dimensional complex, projective Hilbert space $\mathcal{H}$ [Nielsen and Chuang 2000; Rieffel and Polak 2000; Mermin 2007; Gruska 1999; Lanzagorta and Uhlmann 2008]. Qubits are fundamental building blocks for all quantum informational processes [Rieffel and Polak 2000; Mermin 2007; Gruska 1999; Lanzagorta and Uhlmann 2008]. A qubit can be in two observable states corresponding to the two dimensions of the Hilbert space that models them. Further, any two observable states of a qubit form an orthonormal basis of $\mathcal{H}$. Typically in quantum computation, one speaks of the computational basis of $\mathcal{H}$, which is denoted as $|0\rangle$ and $|1\rangle$ in the Dirac notation. Elaborating the linear algebra of $\mathcal{H}$, the computational basis for the Hilbert space of a qubit consists of the two states

$$|0\rangle = \begin{pmatrix} 1 \\ 0 \end{pmatrix} \quad \text{and} \quad |1\rangle = \begin{pmatrix} 0 \\ 1 \end{pmatrix}.$$

Unlike classical bits, qubits can be in a superposition of these two basis states. This quantum superposition represents a weighted "average," where the weights are complex numbers. Hence, it is not immediately obvious as to what practically useful interpretation one can give a quantum superposition. However, axioms of quantum mechanics have proven the practical usefulness of the following interpretation for a quantum superposition; it encodes information about the probability with which it will be measured to be in one of the basis states of the qubit. Measurement of qubits is a particular type of quantum mechanical operation that will be discussed in Section 2.2.

An arbitrary quantum superposition in $\mathcal{H}$ (from now on the terms quantum superposition and qubit will be used interchangeably) is expressed in Dirac notation as follows [Nielsen and Chuang 2000; Deutsch and Jozsa 1992]:

$$|\Psi\rangle = \alpha\,|0\rangle + \beta\,|1\rangle = \begin{pmatrix} \alpha \\ \beta \end{pmatrix}, \tag{1}$$

where α and β are complex numbers [Nielsen and Chuang 2000; Deutsch and Jozsa 1992]. Furthermore, $|\alpha|^2$ and $|\beta|^2$ are the probabilities of measuring $|\Psi\rangle$ in the basis

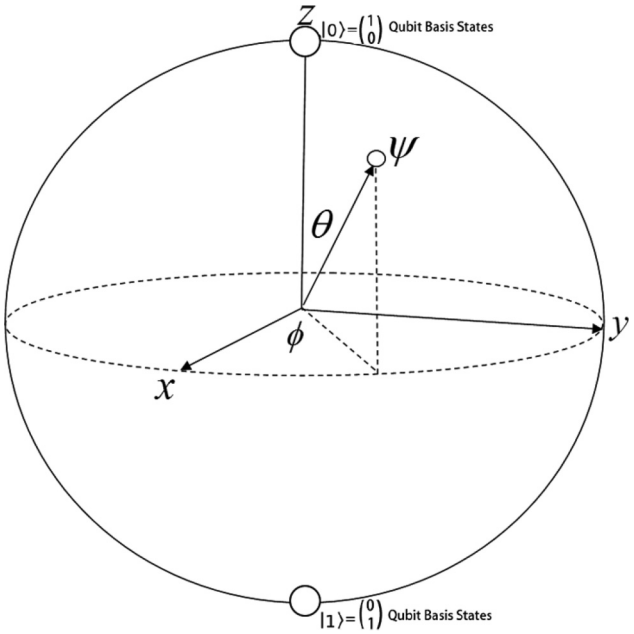

Fig. 1. Complex projective Hilbert space of the state of a qubit visualized as the Bloch sphere, with the qubit states $|0\rangle$ and $|1\rangle$ represented as diametrically opposite points on it [Nielsen and Chuang 2000].

states $|0\rangle$ and $|1\rangle$, respectively. Hence, $|\alpha|^2 + |\beta|^2 = 1$. By Euler angle decomposition, Equation (1) can be rewritten as

$$|\Psi\rangle = e^{i\gamma}\left(\cos\frac{\theta}{2}|0\rangle + e^{i\varphi}\sin\frac{\theta}{2}|1\rangle\right), \tag{2}$$

where θ, γ, and φ are real numbers. After applying quantum measurement, which will be explained in Section 2.2, the effect of γ becomes negligible. Hence, the term $e^{i\gamma}$ is equal to 1 and can be removed from Equation (2). The terms θ and φ define a point on the sphere shown in Figure 1. This is called the Bloch sphere, and its purpose is to visualize the state of a qubit [Nielsen and Chuang 2000; Deutsch and Jozsa 1992].

A general qubit state like $|\Psi\rangle$ in Equation (1) is produced by a unitary operation, the only other quantum operation allowable aside from quantum measurement, which is not unitary. The unitary operator

$$U = \begin{pmatrix} \alpha & -\overline{\beta} \\ \beta & \overline{\alpha} \end{pmatrix}$$

produces $|\Psi\rangle$ by acting on the qubit $|0\rangle$. A unitary operation is simply a rotation of a qubit state to another on the Bloch sphere. In the language of quantum computation, U is referred to as a quantum logic gate, and a sequence of quantum logic gates acting on multiple qubits is referred to as a quantum logic circuit.

Since quantum superposition allows multiple observable states to be processed at once (in this case, they are $|0\rangle$ and $|1\rangle$), it induces parallelism, which is an important tool for handling growing computational demand [Deutsch 1985; Deutsch and Jozsa 1992]. Furthermore, from a hardware point of view, the Deutsch-Jozsa algorithm [Deutsch and Jozsa 1992; Nielsen and Chuang 2000] shown in Figure 2 can be taken as an example to demonstrate how quantum logic circuits can outperform classical ones.

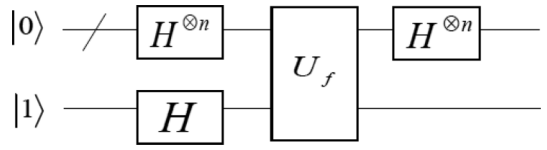

Fig. 2. Deutsch-Jozsa circuit with n number of $|0\rangle$ qubits and $|1\rangle$ qubit as inputs [Nielsen and Chuang 2000].

Figure 2 shows the Deutsch-Jozsa circuit, which consists of Hadamard gates labeled H and is defined as follows for $n = 1$:

$$H = \frac{1}{\sqrt{2}} \begin{pmatrix} 1 & 1 \\ 1 & -1 \end{pmatrix}. \tag{3}$$

The states $|0\rangle$ and $|1\rangle$ will go through the Hadamard gate as follows:

$$H(|1\rangle) = \frac{1}{\sqrt{2}} |0\rangle - \frac{1}{\sqrt{2}} |1\rangle, \tag{4}$$

$$H(|0\rangle) = \frac{1}{\sqrt{2}} |0\rangle + \frac{1}{\sqrt{2}} |1\rangle. \tag{5}$$

The final outcome of this circuit is

$$|\Psi\rangle = \pm |f(0) \oplus f(1)\rangle \frac{|0\rangle - |1\rangle}{\sqrt{2}}. \tag{6}$$

At this stage, a readout of the quantum circuit's outcome has to be made using the principle of quantum measurement. This measurement will produce a probabilistic outcome—namely, each state will be produced with probability one half. This, however, does not mean that the two states exclude each other, as is the case in classical computers. On the contrary, the two states interfere and yield a global property that can be expressed as a function. This is known as quantum interference. By measuring the first qubit only, $f(0) \oplus f(1)$ can be determined with only one evaluation [Nielsen and Chuang 2000; Deutsch and Jozsa 1992]. This would have taken at least two evaluations on classical computers. This effect becomes more evident for a larger n, as a quantum computer would still require a single evaluation regardless of the value of n, but a classical computer would require $2^n/2 + 1$ evaluations [Nielsen and Chuang 2000; Deutsch and Jozsa 1992].

Furthermore, Grover's search algorithm [Grover 1996], which utilizes parallelism via quantum superposition, has been used for image searching. It has been proven that its computational complexity is far better than classical computers' search algorithms, and that it requires fewer numbers of bytes to represent images and obtain them efficiently [Beach et al. 2003; Venegas-Andraca and Ball 2010]. For instance, an unordered database with n entries will take an order of $O(n)$ to search for a particular item in it using classical search algorithms. In comparison, Grover's algorithm takes only $O(\sqrt{n})$ [Grover 1996]. The efficiency of Grover's algorithm as opposed to classical search algorithms becomes more evident as the database grows bigger.

2.2. Quantum Measurement

In comparison to classical physical systems, quantum physical systems are very sensitive to interference from outside the system. One type of outside interference that is discussed in here is the quantum measurement—that is, the act of probing a qubit state for the observable state it is in. This act projects the qubit onto its constituent basis elements, with the length of the projection representing the probability with

which the qubit is going to be seen as that particular basis element. Although this description of quantum measurement may be seen at odds with our macroscopic every day experiences, it is in fact based on extensive data gathered over almost a century of experiments in quantum physics.

Mathematically, quantum measurement can be described by a collection M_m of nonunitary measurement operators [Nielsen and Chuang 2000]. Here, m is the index of the basis state that is being measured. For example, if there are two basis states $|0\rangle$ and $|1\rangle$, there would be two indices, $m = 0$ and $m = 1$. The probability of the measurement producing the observable state m is given by

$$P(m) = \langle \Psi | \, M_m^\dagger M_m \, | \Psi \rangle \, , \tag{7}$$

where † denotes the conjugate transpose of a matrix, $\langle \Psi |$ represents the conjugate transpose of $|\Psi\rangle$, and the state of the quantum system after measurement is

$$\frac{M_m \, | \Psi \rangle}{\sqrt{\langle \Psi | \, M_m^\dagger M_m \, | \Psi \rangle}}. \tag{8}$$

Applying quantum measurement makes the system "collapse" to one of the basis states [Nielsen and Chuang 2000]. For example, consider the qubit state

$$|\Psi\rangle = \alpha|0\rangle + \beta|1\rangle = \begin{pmatrix} \alpha \\ \beta \end{pmatrix}$$

so that

$$\langle \Psi | = \left(\alpha^*, \beta^* \right).$$

The measurement operator

$$M_0 = \begin{pmatrix} 1 & 0 \\ 0 & 0 \end{pmatrix}$$

projects $|\Psi\rangle$ onto the observable state $|0\rangle$ with probability $|\alpha|^2$ since

$$\frac{M_0 \, | \Psi \rangle}{\sqrt{\langle \Psi | \, M_m^\dagger M_m \, | \Psi \rangle}} = \frac{\begin{pmatrix} 1 & 0 \\ 0 & 0 \end{pmatrix} \begin{pmatrix} \alpha \\ \beta \end{pmatrix}}{\sqrt{\alpha^* \alpha}} = \frac{\alpha|0\rangle}{\sqrt{|\alpha|^2}} = |0\rangle$$

with the coefficient $\frac{\alpha}{\sqrt{|\alpha|^2}}$ being a phase term, the effect of which on the measurement outcome is negligible and is typically ignored. On repeated measurements, one gets a probability distribution over the observable states.

The physical, meaningful outcome of quantum measurement can be estimated using quantum state tomography (QuST) [Mastriani 2016]—that is, estimation by maximum likelihood. One of the most common tools for this estimation is the Kalman filter approach, as it is the one that is most robust against noise. Hence, the majority of the algorithms developed in the field of QuIP use it to estimate the results of quantum measurement. It is important to mention that QuST may produce errors, and if errors accumulate throughout the image's pixels, the result may not look visually appealing [Mastriani 2016]. The reader is referred to the cited work for more details.

2.3. Quantum Entanglement

Quantum entanglement is the quantum mechanical property that correlates qubits regardless of how far apart they are [Nielsen and Chuang 2000]. Entanglement can also be defined as the ability of quantum systems to produce the same physical result

when each of them is measured [Gisin 2014]. In other words, knowing the state of one qubit permits one to realize the state of the other qubit without physically interacting with it. Hence, quantum measurement on bipartite entangled systems needs to be done only once. In this sense, quantum entanglement allows one to gain information about the entire quantum system without gaining any information about the subsystems composing it [Susskind 2015].

The tensor product is the appropriate mathematical formalism for discussing quantum entanglement. Like the more commonly used Cartesian product, the tensor product, denoted by the symbol $\otimes$, describes a system that is made of multiple subsystems, such as an image of $n \times m$ pixels. In the case of quantum systems, it describes a system of larger Hilbert space that is constructed from smaller sub-Hilbert spaces. Although the formal definition of a tensor product invokes quotient groups of free groups and categorical language, at the calculation level it has following definition for qubits:

$$|0\rangle \otimes |0\rangle = \begin{pmatrix} 1 \\ 0 \end{pmatrix} \otimes \begin{pmatrix} 1 \\ 0 \end{pmatrix} = \begin{pmatrix} 1 \begin{pmatrix} 1 \\ 0 \end{pmatrix} \\ \\ 0 \begin{pmatrix} 1 \\ 0 \end{pmatrix} \end{pmatrix} = \begin{pmatrix} 1 \\ 0 \\ 0 \\ 0 \end{pmatrix}$$

with other combinations of qubit tensors calculated similarly. The tensor product in the case of Hilbert space is bilinear, in contrast to the linearity of the Cartesian product. In terms of scalar multiplication, the latter satisfies the equation

$$\lambda(\alpha, \beta) = (\lambda\alpha, \lambda\beta),$$

with scalar λ and qubits α and β in $\mathcal{H}$. In contrast, the tensor product behaves as follows

$$\lambda(\alpha \otimes \beta) = (\lambda\alpha \otimes \beta) = (\alpha \otimes \lambda\beta).$$

Hence, the tensor product is a more general form of product than the Cartesian one, and this generality is the source of quantum entanglement. The following example illustrates this further. Consider two qubits

$$\alpha = a_1 |0\rangle + a_2 |1\rangle, \quad \beta = b_1 |0\rangle + b_2 |1\rangle$$

so that $|a_1|^2 + |a_2|^2 = 1$ and $|b_1|^2 + |b_2|^2 = 1$. Further,

$$\alpha \otimes \beta = a_1 b_1 (|0\rangle \otimes |0\rangle) + a_1 b_2 (|0\rangle \otimes |1\rangle) + a_2 b_1 (|1\rangle \otimes |0\rangle) + a_2 b_2 (|1\rangle \otimes |1\rangle)$$

with $|a_1 b_1|^2 + |a_1 b_2|^2 + |a_2 b_1^2| + |a_2 b_2|^2 = 1$. This is the general state of the two qubits when considered as a joint quantum system. Consider next the case where values of $a_i b_j$ are chosen so that

$$\alpha \otimes \beta = \frac{1}{\sqrt{2}} (|0\rangle \otimes |0\rangle) + \frac{1}{\sqrt{2}} (|1\rangle \otimes |1\rangle) = \frac{1}{\sqrt{2}} |00\rangle + \frac{1}{\sqrt{2}} |11\rangle .$$

To be more specific,

$$\alpha \otimes \beta = (a_1 |0\rangle + a_2 |1\rangle) \otimes (b_1 |0\rangle + b_2 |1\rangle) = a_1 b_1 |00\rangle + a_1 b_2 |01\rangle + a_2 b_1 |10\rangle + a_2 b_2 |11\rangle$$

so that

$$a_1 b_1 |00\rangle + a_1 b_2 |01\rangle + a_2 b_1 |10\rangle + a_2 b_2 |11\rangle = \frac{1}{\sqrt{2}} |00\rangle + \frac{1}{\sqrt{2}} |11\rangle .$$

Then, the following four equations are obtained

$$a_1 b_1 = \frac{1}{\sqrt{2}}, \tag{9}$$

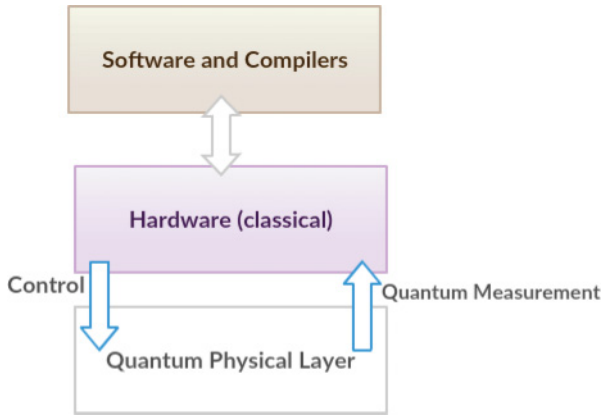

Fig. 3. General configuration of the quantum-classical interface, which is recreated from Reilly [2015].

$$a_2 b_2 = \frac{1}{\sqrt{2}}, \tag{10}$$

$$a_1 b_2 = 0, \tag{11}$$

$$a_2 b_1 = 0. \tag{12}$$

Equations (11) and (12) imply that $a_1 = 0$ or $b_1 = 0$ or $a_2 = 0$ or $b_2 = 0$. However, Equations (9) and (10) imply that $a_1 \neq 0$, $b_1 \neq 0$, $a_2 \neq 0$, and $b_2 \neq 0$. But there exist no complex numbers a_1, a_2, a_3, and a_4 that simultaneously satisfy all Equations (9) through (12). Hence, the quantum state $\frac{1}{\sqrt{2}}|00\rangle + \frac{1}{\sqrt{2}}|11\rangle$ cannot be factored or expressed as the tensor product of two distinct quantum states α and β, and therefore it is entangled.

Although some quantum algorithms, such as Shor's algorithm, generate quantum entanglement during their execution, it is generally not fully understood whether this is the cause of the computational efficiencies exhibited by these algorithms [Kendon and Munro 2006]. However, other applications of quantum information processing are entirely dependent on quantum entanglement for functioning. For example, in quantum teleportation [Bennett et al. 1993], two entangled qubits are used to transmit one bit of classical information across a classical communication channel without actually transmitting the qubits. In addition, the Ekert quantum key distribution (QKD) protocol utilizes quantum entanglement for provably secure exchange of keys for private communication [Ekert 1991].

2.4. Quantum-Classical Interface

Given a quantum computer, the question of programming it is of obvious importance. This brings the issue of the quantum-classical interface. To elaborate further, in any quantum machinery, a key component is the quantum-classical interface, which is an interface between the qubits that contain quantum information and the classical hardware. Figure 3 shows an abstraction of one possible configuration for the quantum-classical interface. This interface allows reading and controlling information that is passed to and from the qubits in the quantum physical layer. The classical circuits involved in the controlling process include digital-to-analogue converters (DACs), analogue-to-digital converters (ADCs), amplifiers (Amps), arbitrary waveform

generators (AWGs), and multiplexers (MUXs) [Reilly 2015]. Quantum measurement is performed between the classical hardware and the quantum physics layer, as seen in Figure 3. Before quantum algorithms are executed, they are first compiled on a quantum computer. After compiling, the quantum algorithms have to be downloaded to the quantum-classical interface. As simple quantum systems are combined to construct larger ones, new challenges are imposed, and this is what makes the quantum-classical interface an active research area that supports the advances of quantum computing technology [Reilly 2015].

2.5. Quantum Frequency and Wavelet Domain Transforms

Fourier transform (FT) [Riley et al. 2006] is a useful mathematical technique to reduce the complexity of engineering problems, such as the ones found in the field of image processing, including reconstruction and compression [Gonzalez and Woods 2007]. Typically, this reduction of complexity amounts to insightful expression of the stated problem in a simpler format so that the solutions are approachable. For instances of such simplifications in image processing, refer to Dubey et al. [2014]. In general, the discrete version of FT (DFT) is represented by the following equation:

$$y_k = \frac{1}{N} \sum_{j=0}^{N-1} x_j e^{2\pi ijk/N}, \tag{13}$$

where x_j is a vector of complex numbers, N is the number of samples, and k is the number of cycles [Nielsen and Chuang 2000]. Note that this equation represents a linear transformation from one basis representation to another. Typically, this transformation is such that the attributes of the function and/or the variables become simpler to analyze in some appropriate context.

Quantum Fourier transform (QFT) does the same transformation as FT, but it is applied on the states themselves instead of the stored data [Nielsen and Chuang 2000], as shown in the following equation:

$$|j\rangle \rightarrow \frac{1}{N} \sum_{j=0}^{N-1} x_j e^{2\pi ijk/N} |k\rangle . \tag{14}$$

It is a unitary operation, and hence it can be implemented on quantum computers. Hadamard gates are used to implement QFT [Nielsen and Chuang 2000].

The computational complexity of fast Fourier transform (FFT), which is a classical algorithm for computing DFT, is $O(n2^n)$ gates when acting on $N = 2^n$ elements. Here, n represents the number of bits. On the other hand, the complexity of QFT is $O(n^2)$ gates [Nielsen and Chuang 2000], where now n represents the number of qubits. This means that QFT requires exponentially less operations than FFT. Caraiman and Manta [2013] attempted to filter an image using QFT and proved that it is, indeed, exponentially faster than its classical counterpart.

Quantum wavelet transforms (QWTs) expose the image in a multiscale structure that is usually expressed as a pyramid. It is a useful tool for image processing generally and image compression particularly. In Fijany and Williams [1998], two of the classical wavelet transforms (WTs), namely Haar and Daubechies $D^{(4)}$, were transformed into quantum circuits, and the rest of the operations were expressed as dot products, direct products, and direct sums of unitary matrices. Since many operations cannot be directly converted to the quantum domain, as they are not typically unitary, the authors exploit qubit permutation matrices. The authors also introduce new quantum logic gates, such as the qubit swap gate. They also described three quantum circuits for Daubechies

$D^{(4)}$ WT, and they showed that its kernel can be implemented using a QFT circuit. The derivations helped to point out the differences of the classical operations and their quantum counterparts. The authors believe that the quantum permutation matrices have a major role to play in the efficient implementation of these circuits and should be explored further. However, they find that "the operations that are easy and inexpensive to implement classically are not always easy and inexpensive to implement quantum mechanically, and vice versa."

Like FT, the discrete cosine transform (DCT) converts a signal from the spatial domain to the frequency domain. It was first proposed by Ahmed et al. [1974], and its applications to image compression were first developed by Chen and Pratt [1984]. For a given vector $x(n)$, $n = 0, 1, 2, \ldots, N$ of real numbers, there are four different types of DCTs [Zhou et al. 2015a; Klappenecker and Rotteler 2001; Wang and hunt 1983]:

—*Type I*:

$$X(k) = \sqrt{\frac{2}{N}}\alpha(k)\sum_{n=0}^{N}\alpha(n)x(n)\cos\frac{kn\pi}{N}, \quad k = 0, 1, \ldots, N$$

with

$$\alpha(k) = \begin{cases} \frac{1}{\sqrt{2}} & k = 0 \text{ or } N \\ 1 & \text{otherwise} \end{cases}$$

and

$$\alpha(n) = \begin{cases} \frac{1}{\sqrt{2}} & n = 0 \text{ or } N \\ 1 & \text{otherwise.} \end{cases}$$

—*Type II*:

$$X(k) = \sum_{n=0}^{N-1}\alpha(n)x(n)\cos\frac{(2k+1)n\pi}{2N}, \quad k = 0, 1, \ldots, N-1$$

with

$$\alpha(n) = \begin{cases} \sqrt{\frac{1}{N}} & n = 0 \\ \sqrt{\frac{2}{N}} & \text{otherwise.} \end{cases}$$

—*Type III*:

$$X(k) = \alpha(k)\sum_{n=0}^{N-1}x(n)\cos\frac{k(2n+1)\pi}{2N}, \quad k = 0, 1, \ldots, N-1$$

with

$$\alpha(k) = \begin{cases} \sqrt{\frac{1}{N}} & k = 0 \\ \sqrt{\frac{2}{N}} & \text{otherwise.} \end{cases}$$

—*Type IV*:

$$X(k) = \frac{2}{N}\sum_{n=0}^{N-1}x(n)\cos\frac{(2k+1)(2n+1)\pi}{2N}, \quad k = 0, 1, \ldots, N-1$$

All four types of DCT were extended to the quantum domain by Klappenecker and Rotteler [2001]. DCT usually takes $O(NLogN)$ operations. However, on quantum computers, it can take as little as $O(Log^2N)$ operations.

3. QUANTUM IMAGE STORAGE, RETRIEVAL, AND COMPRESSION

With the recent advancements in sensor technologies, the quality of images have improved dramatically, thus increasing the demand for efficient storage and retrieval. Although high-quality images are required to provide better results in image processing tasks, such as enhancement and segmentation, the processing of such visual big data requires obtaining and saving as much information, which makes the demand for efficient storage even more compelling.

In classical computers, a red, green, blue (RGB) color image is represented using 24 bits, 8 bits per color channel. From the perspective of real-world applications, for example, the number of the surveillance cameras in the streets of the United Kingdom is estimated to be between 4 and 5.9 million.[1] These cameras work 24/7, and each camera captures, on average, 30 frames per second [Ghosh 2013]. Therefore, the total number of frames collected from all cameras within 7 days is $4{,}000{,}000 \times 300 \times 7 \times 24 \times 60 \times 60 = 725{,}760 \times 10^9$ frames. Again, this result leads to the topic of processing visual big data and the challenges that make the classical computers inflexible for such growing needs. In addition, this is not the only problem for classical computers; most of the classical algorithms have overwhelming computational complexity due to the restrictions of classical computers' architecture [Venegas-Andraca and Ball 2010]. Classical memory cells are independent of each other, and so is the information that is stored within them. Hence, the only way to correlate the values is either by directly storing correlation values or by executing algorithms to calculate the correlation values from the stored ones [Venegas-Andraca and Ball 2010]. For instance, saving the binary information of an image's pixels in memory cells is not enough; the spatial distribution of the pixels is needed as well to fully reconstruct the image. Moreover, in addition, there could be other task-specific parameters that may also be required for performing image analysis accurately. This not only requires a large storage space but also a considerable amount of time for retrieving all relevant data and information. For example, performing a search algorithm to retrieve n vertices of an image from an array of size m would take $O(n)$ operations [Venegas-Andraca and Ball 2010]. Further, it becomes even harder since the mapping between pixels and vertices cannot be located without additional supplementary information.

From a quantum information processing point of view, there has been considerable research effort in the literature to improve image storage and retrieval algorithms [Li et al. 2014; Yan et al. 2014; Li et al. 2013a; Venegas-Andraca and Ball 2010; Zhang et al. 2013c]. These methods exploit the fact that a single qubit, which can store both 0 and 1 with certain probability, is capable of storing much more information than a single bit. Moreover, quantum entanglement can correlate all saved pixel values, which allows efficient storage consumption.

The most famous algorithms for quantum image storage and retrieval are flexible representation of quantum images (FRQI) [Quang et al. 2009], qubit lattice [Venegas-Andraca and Bose 2003b], entangled image [Venegas-Andraca and Ball 2010], and real ket [Latorre 2005]. In the qubit lattice model [Venegas-Andraca and Bose 2003b], every pixel in the image is represented as a qubit. In other words, the image is considered as a two-dimensional array of qubits. On one hand, this makes it easier to extend the classical image processing algorithms to the quantum domain. But on the other hand, this does not improve the performance by much. In addition, this model allows storing the information directly without processing them as RGB channels. Since the range of qubits' angle parameter is not provided, the presentation of this model becomes complex [Venegas-Andraca and Bose 2003b].

[1]This number was reported by the BBC news based on the British Security Industry Association (BSIA) estimates on January 26, 2015 (http://www.bbc.com/news/uk-30978995).

To recover the image's information after storing it, binary data stored in the computer memory must be read. This means that independent measurements must be applied on each pixel and hence on each memory cell. Therefore, applying projection operators will give probabilistic results for the pixels of the image, and it may not be reliably reconstructed. Correlating the image's pixels using entanglement provides a reliable tool to determine their location and construct the image. The entangled image model [Venegas-Andraca and Ball 2010] is designed based on this principle. It is similar to the qubit lattice model and has similar performance, but it uses the entangled state of quantum mechanics to represent relationships between image pixels.

The real ket model performs image quartering iteratively and builds a balanced quadtree index, and the images are represented as quantum states having grey levels as its coefficients [Latorre 2005]. It has better performance than the qubit lattice and entangled image models because in the latter two models, an image is simply represented as a two-dimensional array of qubits, which makes their performance similar to classical digital image processing. However, the real ket model performs image quartering iteratively and builds a balanced quadtree index [Zhang et al. 2013c].

Finally, the most famous and most widely used representation for quantum digital images is the FRQI [Yan et al. 2014; Le et al. 2010], which was proposed by Quang et al. [2009] and Le et al. [2011b]. FRQI was developed to aid the extension of the classical image processing algorithms to the quantum domain [Quang et al. 2009]. In FRQI, the color and position of every pixel in the image are represented, and the image is in a normalized state. The information is then integrated into a quantum state by applying the tensor product as follows:

$$|I(n)\rangle = \frac{1}{2^n} \sum_{i=0}^{2^{2n}-1} |c_i\rangle \otimes |i\rangle \tag{15}$$

such that

$$|c_i\rangle = \cos\theta_i \,|0\rangle + \sin\theta_i \,|1\rangle\,, \tag{16}$$

$$\theta_i \in [0, \pi/2], i = 1, 2, \ldots, 2^{2n} - 1, \tag{17}$$

where θ is the vector of angles encoding the colors [Quang et al. 2009] and $|i\rangle$ indicates the corresponding positions. As mentioned before, quantum measurement must be applied to extract the necessary information for retrieving and constructing a quantum image. However, general quantum states have complex coefficients, which makes the probability distributions insufficient to understand the states of qubits clearly. This problem is not present in FRQI because it contains only real coefficients, which makes it possible to retrieve all information about the state of any qubit in the image [Quang et al. 2009]. FRQI has better performance than the qubit lattice and entangled image models and has similar performance to that of the real ket model, as both of them can process all pixels of the image simultaneously. However, FRQI maintains a two-dimensional qubit sequence, which is entangled, and the greyscale information is stored as the probability amplitude of a single qubit in the sequence. This is what makes it, thus far, the most suitable and flexible model for representing quantum images and designing QuIP algorithms. Hence, researchers have focused on the FRQI model and have improved on it [Zhang et al. 2013c]. In addition, there are many algorithms designed based on FRQI. For instance, quantum image compression (QIC) is usually used with FRQI to reduce the number of simple operations. It is reported that the compression effect ranges from 6.67% to 31.62% [Quang et al. 2009]. Before FRQI emerged, an attempt to achieve image compression on quantum computing was made

by Latorre [2005], which demonstrated promising results but was not as effective as the results obtained when FRQI was utilized. FRQI has not only shown efficiency in compression but has also indicated promising results in quantum binary image search based on probability distributions [Yan et al. 2012], as well as representing and producing movies on quantum computers [Iliyasu et al. 2011]. The notion of "quantum player" was also introduced by Iliyasu et al. [2011], which manipulates the contents of the key frames to interpolate the missing viewing frames that depict the motion and the scenes more effectively and makes them appear smoother. This was done by utilizing geometric transforms on quantum images (GTQI) [Iliyasu et al. 2012], simple motion operation (SMO) [Iliyasu et al. 2011], and color transformations on quantum images (CTQI) [Le et al. 2011a]. The method still requires improvements, as Iliyasu et al. [2011] considered improving FRQI to represent geometry and movements more efficiently, and also to adjust the representation in such a way that it can incorporate sound.

An extension to the FRQI model was proposed for the multicolor domain called *multichannel representation for quantum images* (MCRQI) [Sun et al. 2011; Bun et al. 2013a]. The aim of this model was to represent and process images in RGB color space. The MCRQI model is represented as

$$|I(n)_{mc}\rangle = \frac{1}{2^{n+1}} \sum_{i=0}^{2^{2n}-1} \left|C^i_{RGB\alpha}\right\rangle \otimes |i\rangle \,, \tag{18}$$

where $|C^i_{RGB\alpha}\rangle$ represents the color information encoding the RGB channel and is defined as

$$\begin{aligned} \left|C^i_{RGB\alpha}\right\rangle = {} & \cos\theta^i_R\,|000\rangle + \cos\theta^i_G\,|001\rangle + \cos\theta^i_B\,|010\rangle + \cos\theta_\alpha\,|011\rangle \\ & + \sin\theta^i_R\,|100\rangle + \sin\theta^i_G\,|101\rangle + \sin\theta^i_B\,|110\rangle \sin\theta_\alpha\,|111\rangle \,, \end{aligned} \tag{19}$$

where $\theta^i_R, \theta^i_G, \theta^i_B \in [0, \pi/2]$ represents the three angles that encode the RGB channels of the color image [Sun et al. 2011; Bun et al. 2013a]. Based on this representation, multichannel information operations on quantum images was proposed by Sun et al. [2014]. The authors designed quantum circuits for operations, such as channel swapping and alpha blending, using simple gates, which include NOT, CNOT, Toffoli, and rotation gates. The complexity was independent of the size of the image, and it was believed that these operations would help the future directions of research be extended to quantum image geometric transformation and quantum image watermarking [Sun et al. 2014].

Based on the analysis of the previously discussed quantum image representation techniques, Zhang et al. [2013c] proposed a novel enhanced quantum representation (NEQR) technique. According to NEQR, an image is represented using the following equation:

$$|I\rangle = \frac{1}{2^n} \sum_{YX=0}^{2^{2n}-1} |f(X,Y)\rangle\,|YX\rangle \,. \tag{20}$$

According to Zhang et al. [2013c], NEQR is an improved version of FRQI. Whereas FRQI uses the basis states of the qubits to represent their probability amplitudes, NEQR uses them to store the greyscale value of each pixel. Hence, Zhang et al. [2013c] state that NEQR can perform all of the following greyscale operations:

—*Complete color operations* (CC): Operations that deal with all the pixels in the image or a certain area

—*Partial Color operations* (PC): Operations that deals only with certain greyscale values
—*Color statistical operations* (CS): Operations that perform certain statistical computations based on the greyscale information in the image, such as a greyscale histogram.

However, FRQI can only perform CC because it saves greyscale information in one qubit only. Therefore, it becomes difficult to separate pixels with different greyscale values [Zhang et al. 2013c]. In addition, the original digital image can be accurately retrieved from NEQR, and unlike FRQI, it is not probabilistic. Moreover, NEQR avoids complex quantum rotation operations, which reduces the computational complexity. For an image represented by $2^n \times 2^n$ pixels, the computational complexity of FRQI is $O(2^{4n})$ [Zhang et al. 2013c]. On the other hand, the computational complexity for NEQR is $O(2^n)$, which achieves quadratic speedup. In terms of compression, NEQR achieves a higher compression ratio than FRQI by approximately 1.5 times. The limitation of NEQR is the trade-off between having extra quantum storage and significant performance improvement.

Other algorithms for storing and retrieving images with color information include the normal arbitrary quantum superposition state (NAQSS) [Li et al. 2013b], where the algorithms typically use $(n+1)$ qubits to store the pixels. In this case, n represents the color and coordinates of 2^n pixels, and the extra pixel represents segmentation information required to improve the image's segmentation.

Further work on improving storage and retrieval of color images was proposed in Song et al. [2013]. A multichannel color quantum image based on the phase transform (CQIPT) algorithm was developed to easily process color transformations, transparency, adjustments, and geometric transforms using phase gates. In addition, the algorithm was designed to ease other quantum processes that might require phase encoding, which is usually required for image geometric transformations and image security. The feasibility of the algorithm was tested, and corresponding circuits were designed. From a performance point of view, the complexity of the algorithm was similar to that of MCRQI. However, CQIPT was more flexible than MCRQI for random-phase functions that could be used for encryption.

A demonstration of the use of quantum entanglement to store and retrieve grey and colored images was explained in Li et al. [2014]. The authors employed a two-qubit entangled quantum state to represent three pixels and a three-qubit entangled quantum state to represent five pixels. First, the two-qubit entangled quantum state is designed as

$$|\chi_2\rangle = a_0\,|00\rangle + a_1\,|01\rangle + a_2\,|10\rangle + a_3\,|11\rangle\,. \tag{21}$$

If there are three different angles constituting θ_1, θ_2, and θ_3, and if $a_0 = \cos\theta_1 \cos\theta_2$, $a_1 = \cos\theta_1 \sin\theta_2$, $a_2 = \sin\theta_1 \cos\theta_3$, and $a_3 = \sin\theta_1 \sin\theta_3$, the equation becomes

$$|\chi_2\rangle = \cos\theta_1 \cos\theta_2\,|00\rangle + \cos\theta_1 \sin\theta_2\,|01\rangle + \sin\theta_1 \cos\theta_3\,|10\rangle + \sin\theta_1 \sin\theta_3\,|11\rangle\,. \tag{22}$$

If the states $|0\rangle$ and $|1\rangle$ are taken as a common factor, then

$$|\chi_2\rangle = (\cos\theta_1 \cos\theta_2\,|0\rangle + \sin\theta_1 \cos\theta_3\,|1\rangle)\,|0\rangle + (\cos\theta_1 \sin\theta_2\,|0\rangle + \sin\theta_1 \sin\theta_3\,|1\rangle)\,|1\rangle\,. \tag{23}$$

Therefore, the probability of obtaining the state $|0\rangle$ is

$$P_0 = \cos^2\theta_1 \cos^2\theta_2 + \sin^2\theta_1 \cos^2\theta_3, \tag{24}$$

and the probability of obtaining state $|1\rangle$ is

$$P_1 = \cos^2\theta_1 \sin^2\theta_2 + \sin^2\theta_1 \sin^2\theta_3. \tag{25}$$

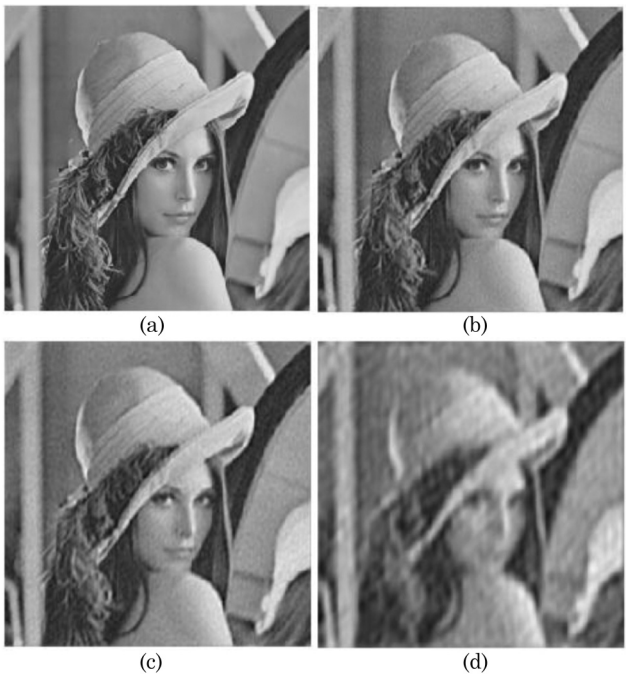

Fig. 4. (a) Original image. (b) QFT with a low compression factor. (c) QFT with a medium compression factor. (d) QFT with a high compression factor. Increasing the compression factor of QFT causes the image to look distorted [Li et al. 2014].

Finally,

$$|\chi_2\rangle = \sqrt{P_0}\,|0\rangle\,|u\rangle + \sqrt{P_1}\,|0\rangle\,|v\rangle\,. \tag{26}$$

In a similar way, a three-qubit entangled quantum state is derived and represented as

$$\begin{aligned}|\chi_3\rangle \;=\; &(\cos\theta_1\cos\theta_2\,|0\rangle + \sin\theta_1\cos\theta_3\,|1\rangle)\,|0\rangle\,|u\rangle + (\cos\theta_1\sin\theta_2\,|0\rangle \\ &+ \sin\theta_1\sin\theta_3\,|1\rangle)\,|1\rangle\,|v\rangle\,,\end{aligned} \tag{27}$$

where $|\chi_3\rangle$ represents five colors. Similarly, $|\chi_5\rangle$ can be derived to represent seven colors. In fact, any $|\chi_n\rangle$ system can be derived, which could represent $2n-1$ colors. In addition, these entangled states also have a compression effect. For instance, a two-qubit entangled system has a compression rate of 3/2. Similarly, a three-qubit entangled system has a 5/3 compression ratio. Generally, an n-qubit entangled system will have a $(2n-1)/n$ compression rate. This property was exploited in Li et al. [2014] to enhance this compression effect by incorporating QFT. Figure 4 shows the compression effect of QFT. The compression rate of QFT can reach as high as 59.2, and the PSNR of the compressed image is 24.5dB, indicating higher image distortion for a high compression rate. The distortion effect can also be clearly noticed in the images that have a high compression rate, as shown in Figure 4. Moreover, Li et al. [2014] stated that three-qubit entangled states should be applied at most, as the complexity of the realization increases dramatically for m-qubit, where $m > 3$.

The previously discussed work of Li et al. [2014] was inspired by the work done in Li et al. [2013a], in which a quantum image storage, retrieval, compression, and segmentation algorithm was proposed. An algorithm that can store an image of n pixels and m colors using only $2n+m$ qubits was designed. The computational complexity of the proposed search algorithm was $O(t\sqrt{n})$, where t is the number of targets to be

Table I. Comparison Between Quantum Image Storage, Retrieval, and Compression Methods

Method	Computational Complexity	Compression Rate	Type of Image
FRQI [Yan et al. 2014]	$O\left(2^{4n}\right)$	6.67% to 31.62%	Colored
NEQR [Zhang et al. 2013c]	$O\left(2^{n}\right)$	1.5 times higher than FRQI	Colored
Li et al. [2014]	Better than Li et al. [2013a]	$(2n-1)/n$	Colored
Li et al. [2013a]	$O(t\sqrt{n})$	n_1/n_2	Colored

segmented and n is the number of pixels. The compression ratio is

$$R = n_1/n_2, \tag{28}$$

where n_1 represents the number of pixels of the original image and n_2 represents the number of pixels of the compressed image. The work in Li et al. [2014] showed a better compression rate than the work in Li et al. [2013a] while preserving as much details as possible. However, the computational complexity of the algorithm presented in Li et al. [2014] was better than the one presented in Li et al. [2013a], as the latter's performance decreases dramatically if more than three qubits are used. A comparison between FRQI, NEQR, Li et al. [2013a], and Li et al. [2014] is summarized in Table I.

Storage and retrieval algorithms can be optimized further if they are designed for specific types of images. For instance, Venegas-Andraca and Ball [2010] designed an image storage and retrieval algorithm for binary geometrical shapes. They proposed saving the image in an array of size n qubits. Each qubit contains x and y parameters, which represent "grid points" of a two-dimensional image. These qubits are initially at state $|0\rangle$. The authors extended the classical binary image representation to qubits. In other words, white points were associated with state $|0\rangle$, and black ones were associated with state $|1\rangle$. For instance, and according to Venegas-Andraca and Ball [2010], if it were required to save a triangle, each vertex could be represented by setting $|1\rangle$ to its corresponding qubit. Then, Grover's search algorithm was used for image retrieval. Searching for a $|1\rangle$ in an array of size n would have taken a computational complexity of $O(n)$ on a classical computer. However, it only takes $O(\sqrt{n})$ on a quantum computer using Grover's algorithm. Difficulties arise if many shapes are saved; if it is desired to save two triangles, there is no way to know which vertices belong to which triangle. In this case, entanglement can be applied by establishing nonlocal correlations between qubits that represent vertices of the same triangle. This means that vertices belong to the same triangle only if they are entangled. Venegas-Andraca and Ball [2010] followed this principle and applied it to real-world images. The model was tested on an image of overlapping ladders, which is similar to the case of overlapping chairs shown in Figure 5, and each one was detected successfully.

Although the method presented by Venegas-Andraca and Ball [2010] was not as complicated as the ones presented by Li et al. [2014] and Li et al. [2013a], it solved one of the important challenges for image edge detection and segmentation, which is detecting overlapping and nonoverlapping objects. Inspired by the qubit lattice model, Yuan et al. [2014b] proposed a method for simple quantum representation (SQR) of infrared images, which was based on the fact that infrared images reflected infrared radiation energy of objects [Yuan et al. 2014b]. Unlike the qubit lattice model, SQR did not store color information in its angle parameter. Instead, it stored the radiation energy value of each pixel. The state of a single qubit is represented as

$$|\psi_{ij}\rangle = \cos\frac{\theta_{ij}}{2}|0\rangle + \sin\frac{\theta_{ij}}{2}|1\rangle, \tag{29}$$

where θ_{ij}, $i = 1, 2, \ldots, N_1$ and $j = 1, 2, \ldots, N_2$ are all real numbers, and they can be used to view the position of $|\psi_{ij}\rangle$ on a Bloch sphere. In addition, θ_{ij} stores the the radiation energy value. According to Yuan et al. [2014b], the advantage of SQR is

Fig. 5. Two overlapping chairs. These overlapping chairs can be detected by making the vertices of the same chair entangled. A similar example of two overlapping ladders is illustrated in Venegas-Andraca and Ball [2010].

that the parameters range is defined, which makes it more convenient to use than the qubit lattice model. As a result, more imaging operations can be performed with SQR more conveniently than performing them with qubit lattice. In addition, it only requires using simple quantum gates, such as a single qubit Hadamard gate [Yuan et al. 2014b], and that results in a low computational complexity.

Thus far, existing algorithms can only represent quantum images in Cartesian coordinates. Therefore, Zhang et al. [2013d] proposed the quantum log-polar image (QUALPI), which can sample images in polar coordinates from a classical image with a complexity that is approximately linear in image size. This algorithm uses three entangled qubits to store three types of information for each pixel: greyscale information, the log-radius position, and the angular position. The advantage that this method offers is the ease of performing geometric transformations, such as symmetry transformation and rotation. Based on this, the Zhang et al. [2013d] also proposed an image registration algorithm that shows quadratic speedup over classical image registration methods.

All of the studied algorithms that are related to quantum image storage, retrieval, and compression showed improvement over the classical method of representing images on classical computers. This is a significant proof that quantum computing can indeed enhance the performance of imaging operations. This has been further proven in Yan et al. [2016]. The authors gathered the mainstream methods of representing images of quantum computers and assessed them in terms of their similarities, differences, shortcomings, and possible applications, if available. The field is still prone to many potential improvements, and attention should be paid to low-level image and video

processing [Yan et al. 2016]. The future of this field is to find a way to represent images that can show better performance than FRQI. This could lead to significant changes in other imaging operations, as there are many other quantum imaging algorithms that are highly dependent on the FRQI, as will be explained in the next sections.

4. QUANTUM IMAGE DENOISING

Image enhancement, particularly image denoising, is critical to further steps in image analysis and understanding, such as in image edge detection. The representation of an image in digital systems requires pipelining the visual signal through various stages between acquisition and storage that can introduce noise (e.g., sensor noise [Patidar et al. 2010; Verma and Ali 2013], digitization noise [Patidar et al. 2010], and transmission noise [Patidar et al. 2010; Verma and Ali 2013]). In addition, the ambient conditions of the environment itself can become an inherent source of noise, such as in foggy images [Verma and Ali 2013] and low-light images [Verma and Ali 2013]. One of the main challenges is to be able to remove noise, of diverse characteristics, from an image while preserving the fine structures of the image content.

Depending on the source, noise can be classified into two main types:

—*Additive:*

$$X[n] = I[n] + N[n], \tag{30}$$

—*Multiplicative:*

$$X[n] = I[n]N[n], \tag{31}$$

where $I[n]$ is the noise-free image, $N[n]$ is the noise, and $X[n]$ is the noisy image. As mentioned previously, regardless of the source of noise, it is desirable to eliminate noise with as much precision as possible while preserving the image structure. Filtering is one of the most common strategies chosen for image enhancement. Image denoising (also sometimes referred to as noise reduction) is a well-known image processing task. Mathematically, it means recovering $I[n]$ from $X[n]$ [Bhattacharyya et al. 2014]. Denoising can be accomplished using either linear denoising filtering or nonlinear denoising filtering [Ghosh 2013]. Linear filtering techniques, which are commonly used particularly for handling additive and multiplicative noise types, are known for their speed but at the compromise of image structure (i.e., the loss of image detail). Common examples of linear filtering include mean filters [Ghosh 2013], nonlocal means [Buades 2005], and anisotropic diffusion [Perona and Malik 1990]. On the other hand, nonlinear filtering techniques, such as the median filter (MF) [Ghosh 2013] and bilateral filter [Tomasi and Manduchi 1998], are effective in preserving image detail while suppressing noise. However, nonlinear modeling of noise characteristics can be complicated and may require recursive modes of operation, therefore increasing the computational demand.

Although vast literature is available for image denoising from a classical point of view, in this review, those denoising techniques with corresponding quantum equivalents are chosen for survey. In this context, MF, which is the simplest and most popularly nonlinear filter, is considered. The MF runs through all of the pixels in an image, replacing them by the median value of their neighboring pixels [Patidar et al. 2010].

$$y(t) = median((x(t - T/2), x(t - T1 + 1), \ldots, x(t), \ldots, x(t + T/2)) \tag{32}$$

As an example, Figure 6 shows pixel values of an image. The values would be rearranged as follows: 15, 16, 17, 19, 20, 21, 23, 24, 25. The median value is 20. Hence, 16 will be replaced by that value.

MF and some of its extensions [Zhou et al. 2010; Patidar et al. 2010; Verma and Ali 2013] are known for working well with images that are corrupted with salt and pepper

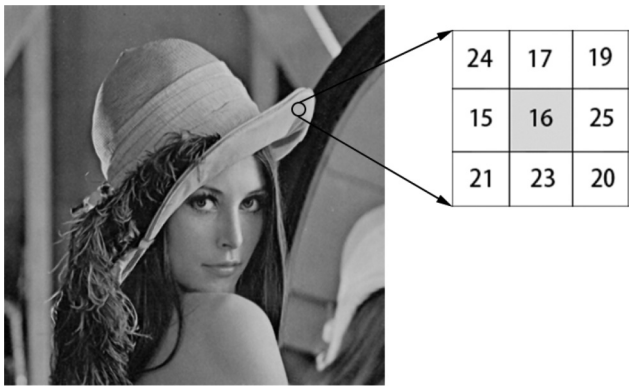

Fig. 6. Example of sample pixel values of a small region in a Lena image. The result of calculating the median of these values is 20, and the value 16 will be replaced with 20.

noise. This classical MF operates on a window of a particular size (typically 3×3 or 5×5). The challenge of choosing an appropriate window size has been addressed in Verma and Ali [2013] and Zhou et al. [2010]. Here, the effect of choosing a large window has been reported to destroy the image structure, whereas a small window does not effectively remove noise. Thus far, no effective rules have been established for selecting an appropriate window size [Zhou et al. 2010]. A more advanced version of the MF is the adaptive median filter (AMF) [Zhou et al. 2010]. This filter updates its window size based on the noise intensity, which leads to better outcomes than the MF with a fixed window size.

Zhou et al. [2010] introduced a quantum collapsing median filter (QCMF). Here, the image pixels are represented by superposition states. If there exists a value $f_1 \in [0, 1]$ that indicates the grey level of a pixel, the superposition of the pixel can be represented as

$$|\Psi\rangle = \omega_0 |0\rangle + \omega_1 |1\rangle , \tag{33}$$

where $\omega_1 = \sqrt{f_1}$, and $\omega_0 = \sqrt{1 - f_1}$, and $|\omega_0^2|$ and $|\omega_1^2|$ are the probabilities of $|0\rangle$ and $|1\rangle$, respectively. Furthermore, if there exists a squared image of $n \times n$, where n is the number of rows and columns, it can be represented as the tensor product of all of its pixels:

$$B_q(x, y) = |\Psi_{n\times n}\rangle \left|\Psi_{(n\times n)-1}\right\rangle \ldots |\Psi_1\rangle = |i_b\rangle , \tag{34}$$

where x and y represent the coordinates. Then, applying the measurement operator from Equations (7) and (8) to Equation (34) causes the noisy pixels to be collapsed to state $|0\rangle$, whereas it causes the nonnoisy pixels to be collapsed to state $|1\rangle$. This yields

$$\frac{M(x, y)B_q}{\sqrt{B_q|M^{+}M(x, y)|B_q}} = \frac{\omega_i|i_M(x, y)\rangle}{\sqrt{\omega_i^2}} = |i_M(x, y)\rangle. \tag{35}$$

It has been shown that with the increase in noise intensity, the filter automatically adjusts its window size starting from 1×1 to 11×11 with an odd number of steps. This filter has a better PSNR than MF and AMF, as shown in Table II. However, the PSNR has barely shown an improvement of 1.1% when compared to that of MF and AMF. Moreover, for an image that is 90% corrupted with noise, QCMF restores most of the image's structure, but there is still a huge amount of enhancement that can be achieved, as shown in Figure 7.

Table II. Comparison of Various Denoising Methods

Method	Noise	PSNR (dB)	SNR (dB)	MSE
MF (5×5)	10%	27.2105	—	—
AMF [Zhou et al. 2010]	10%	33.9918	—	—
QCMF* [Zhou et al. 2010]	10%	38.8864	—	—
QAMF* [Yuan et al. 2013]	10%	36.5379	—	—
Pan et al. [2012]*	10%	—	15	—
LAWF [Parmar and Patil 2013]	8.1dB	17	—	—
BMF [Mastriani 2014a]	5%	35.0436	—	20.3573
QBMF* [Mastriani 2014a]	5%	36.3175	—	15.1819
BI-DTCWT [Fu et al. 2010]	9.72dB	—	11.08	—
Frost Filter [Fu et al. 2010]	9.72dB	—	13.11	—
GenLink [Fu et al. 2010]	9.72dB	—	14.96	—
DTCWT with quantum threshold* [Fu et al. 2010]	9.72dB	—	16.40	—

*Denotes a quantum filter.

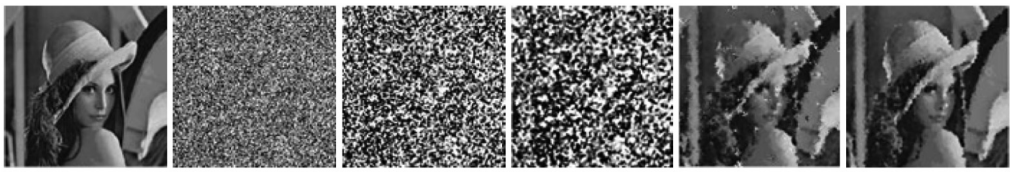

(a) (b) (c) (d) (e) (f)

Fig. 7. (a) A 256×256 original image. (b) Original image corrupted by 90% salt and pepper noise. (c) Corrupted image filtered by a standard MF 3×3. (d) Corrupted image filtered by a standard MF 5×5. (e) Corrupted image filtered by AMF. (f) Corrupted image filtered by the proposed QCMF [Zhou et al. 2010].

Yuan et al. [2013] proposed an alternative quantum version of AMF, called *the quantum adaptive median filter* (QAMF). According to this method, each pixel is transformed into a dual state, which is a superposition of four quantum states:

$$|q(m,n)\rangle = c_{00}\,|00\rangle + c_{01}\,|01\rangle + c_{10}\,|10\rangle + c_{11}\,|11\rangle, \tag{36}$$

where $|c_{00}|^2$, $|c_{01}|^2$, $|c_{10}|^2$, $|c_{11}|^2$ are the probabilities of their respective states, and their summation is equal to 1. If S_{nm} is an $n \times m$ subimage, which is taken from a noisy image and centered at coordinates (n, m), then two variables can be introduced. The first is z_{nm}, which denotes the intensity value at coordinate (n, m). The second is z_{med}, which denotes the median of intensity values in S_{nm}. Both of these variables $\in [0, 1]$. In addition, $f(z)$ is defined as

$$f(z) = sin^2(\pi z), \tag{37}$$

where z can be z_{nm} or z_{med}. $f(z) \in [0, 1]$. Therefore, by using conditional probability, the following relations can be obtained:

$$|c_{11}|^2 = f(z_{med}) \cdot f(z_{nm})$$

$$|c_{10}|^2 = f(z_{med}) \cdot (1 - f(z_{nm}))$$

$$|c_{01}|^2 = (1 - f(z_{med})) \cdot f(z_{nm})$$

$$|c_{00}|^2 = (1 - f(z_{med})) \cdot (1 - f(z_{nm})).$$

After performing quantum measurement, the output will be in one of the four states: $|00\rangle$, $|01\rangle$, $|10\rangle$, $|11\rangle$. The authors have summarized the output mappings as follows:

(1) If the output is $|11\rangle$, then the value of the pixel is z_{nm}.
(2) If the output of the pixel is $|10\rangle$, then the value of the pixel is z_{med}.
(3) Finally, if the output is either $|00\rangle$ or $|01\rangle$, then the window size must be increased and the comparison is repeated in a loop. The loop terminates either when all of the image's pixels have fallen under the outputs in (1) or (2), or the window size has become bigger than a certain specified value. In that case, the pixels will be replaced by the median value.

The performance of the QAMF was compared to the classical MF at 3×3 and 5×5 window sizes in terms of PSNR and normalized mean square error (NMSE). Results have demonstrated that, even under 50% salt and pepper noise, the QCMF showed a slightly better PSNR under the same noise intensity, as shown in Table II.

In recent years, filter banks have found applications in image processing, particularly in image denoising. The WT is of significant importance in this context. It surpasses FT in the sense that it preserves both time and spatial domains [Parmar and Patil 2013]. WT is a powerful, multiscale analysis tool that can separate the noise component from the original signal. This is done using two main methods: soft threshold and hard threshold [Wang and Li 2007]:

—*Soft threshold*:

$$\eta_s(\omega, T) = \begin{cases} \omega - T & \text{if } \omega \geq T, \\ 0 & \text{if } |\omega| < T, \\ \omega + T & \text{if } \omega \leq -T; \end{cases}$$

—*Hard threshold*:

$$\eta_h(\omega, T) = \begin{cases} \omega & \text{if } |\omega| \geq T, \\ 0 & \text{if } |\omega| < T. \end{cases}$$

After transforming the image to the wavelet domain, any typical denoising filter, such as the MF [Parmar and Patil 2013] or Wiener filter [Parmar and Patil 2013], can be used to remove the seemingly isolated noise. Further, the inverse WT is then applied to reconstruct the original image. For example, in the work of Parmar and Patil [2013], a local adaptive Wiener filter (LAWF) was applied and was demonstrated to have achieved a good PSNR of 17dB under 8.1dB noise intensity, as well as good qualitative visual results.

The QuIP literature shows that WT has been used mostly to reduce quantum noise in medical images. It has been attempted to extend WT to the quantum domain [Wang and Li 2007]. Soft and hard thresholds can be represented as a quantum superposition, as it has a nonlinear, probabilistic mapping [Wang and Li 2007]:

$$|W\rangle = N|0\rangle + S|1\rangle, \tag{38}$$

where $|0\rangle$ denotes a noise state, $|1\rangle$ denotes a signal state, and N and S denote their probability amplitudes, respectively. This superposition collapses to a stationary state once the quantum measurement is applied. Unlike the classical WT, which has a predetermined threshold, QWT has a threshold that is presented as a probability distribution. This is due to the probabilistic nature of the quantum states, and it makes the filter more adaptive to different noise densities. It also reduces pseudo-Gibbs phenomena [Wang and Li 2007]. The downside is that the resulting image appears to be blurry to a certain extent due to the dilation of the edges, as shown in Figure 8.

In a similar study in the quantum domain by Fu et al. [2010], WT was applied to reduce speckle noise in ultrasound images. Fu et al. [2010] introduced a quantum-inspired adaptive threshold in a way similar to Wang and Li [2007]. The noise variance is calculated after applying a log transformation of the image and decomposed using

Fig. 8. (a) Original image. (b) Noisy image. (c) Wavelet denoising by hard a threshold. (d) Wavelet denoising by a quantum threshold [Wang and Li 2007]. The results of both (c) and (d) appear to be blurry.

dual-tree complex wavelet transform (DTCWT) [Fu et al. 2010]. Using the estimated noise variance, the complex coefficients were reduced according to quantum-inspired adaptive threshold function. This was done by taking advantage of the fact that "the magnitudes of high frequency signal coefficients have stronger correlation than those of noise coefficients" [Fu et al. 2010]. Hence, signal and noise coefficients can be distinguished using the following equation:

$$C_{smn} = |Y(s+1, m, n)| \times |Y(s, m, n)|, \tag{39}$$

where $|Y(s, m, n)|$ represents the modulus of complex wavelet coefficient. Similar to Equation (38), Fu et al. [2010] also used the principle of quantum superposition to express C_{smn} as a superposition between noise and signals in the high frequency subband:

$$|C_{smn}\rangle = N\,|0\rangle + S\,|1\rangle. \tag{40}$$

Furthermore, $|C_{smn}\rangle$ can be defined as

$$|C_{smn}\rangle = \cos(NC_{smn} \times p/2)\,|0\rangle + \sin(NC_{smn} \times p/2)\,|1\rangle, \tag{41}$$

where NC_{smn} denotes the normalized C_{smn} and $NC_{smn} \in [0, 1]$. Finally, an inverse DTCWT is applied and the exponential transformation is taken to obtain the despeckled image. Experimental results show that this method demonstrated a better performance compared to other classical methods that are commonly used, such as Frost filter, the GenLik method, and the log wavelet BI-DTCWT method [Fu et al. 2010]. These methods are compared using the SNR, as shown in Table II.

There have been a few attempts in the literature to denoise medical images using other quantum filters. For example, in Brida et al. [2010], an attempt to reduce subshot noise using a novel quantum imaging technique was made. Subshot noise (also known

as Poisson noise) is a type of noise that results from the discrete nature of electric charges [Brida et al. 2010]. It is also associated with photons in optical devices [Brida et al. 2010], such as the ones used in medicine. The problem with medical images is that the patient must be exposed to x-ray photons for a relatively long period of time to extract as much information as possible. However, it is desirable to reduce the patient's exposure to x-ray, which may cause the image to remain underexposed. The technique proposed by Brida et al. [2010] allows images, even if the photon exposure is low, to have an SNR higher than classical imaging techniques. Mainly, the method takes into account strong correlations resulting from quantum entanglement due to parametric down conversion (PDC). As a result, "the image of a weak absorbing object in one branch can be restored by subtracting the spatial noise pattern measured in the other branch" [Brida et al. 2010]. The authors proved that this technique is more powerful, with an SNR 70% higher than its classical counterpart, which is differential classical imaging (DCI).

The previous discussion indicates that the main problem with medical images is the need to extract as much information as possible. In fact, this is mostly the main issue for any type of digital image. The more information that can be obtained about an image, the easier it is to process and denoise. This is a significantly bigger challenge for binary images, as they contain less information than color images, making them harder to denoise [Pan et al. 2012]. Mean filters are the most suitable filters for denoising binary images. The idea behind mean filters is to replace each pixel with the mean value of its neighbors, including itself [Mastriani 2014a]. By referring to Figure 6, the mean of the values would be computed as 20, and pixel 16 would be replaced by that value.

Just like the MF, the choice of window size is often 3×3 or 5×5. The trade-off for choosing a relatively small or large window size is similar to the MF as well. In Mastriani [2014a], attempts were made to denoise an image by decomposing it to the RGB color channels. Further, the bits of each component are represented as computational basis states (CBS), in which a quantum Boolean mean filter (QBMF) is applied. This is done to avoid the problem of quantum measurements, which alters the result of what is being measured, except for the case of CBS. The authors tested their technique on a 512×512 Lena image. Figure 9 shows the results. The results obtained from the Boolean mean filter (BMF) and QBMF are not significantly different, and that could be the result of low noise intensity.

A novel way of denoising binary images without destroying their structure was suggested in Pan et al. [2012]. The method was based on representing the image as a quantum system, in addition to proposing the concepts of noise feature codeword" (NFCW) and noise feature codebook (NFCB) [Pan et al. 2012]. NFCW is represented as

$$NFCW_P = \{\lambda_1, \lambda_2, \lambda_3\}, \tag{42}$$

where these three parameters can be calculated as

$$\lambda_1 = D_H\left(|P_3\rangle, |\chi_3\rangle\right), \tag{43}$$

$$\lambda_2 = D_H\left(|P_5\rangle, |\chi_5\rangle\right) - D_H\left(|P_3\rangle, |\chi_3\rangle\right), \tag{44}$$

$$\lambda_3 = D_H\left(|P_7\rangle, |\chi_7\rangle\right) - D_H\left(|P_5\rangle, |\chi_5\rangle\right), \tag{45}$$

where P is the pixel of the image I with the value υ_p and $|P_n\rangle$ represents the pixels in the image within $n \times n$ window. The same thing applies for $|\chi_n\rangle$. All $|P_n\rangle$ states have the value υ_p. The parameters λ_1, λ_2, and λ_3 represent the amount of pixels, with distances 1, 2, and 3 with respect to pixel P, and their values differ from υ_p [Pan et al. 2012]. D_H

Fig. 9. Denoising a Lena image corrupted with 5% salt and pepper noise using classical BMF and the proposed QBMF [Mastriani 2014a]. QBMF shows slightly better quality than classical BMF.

measures the Hamming distance between $|P_n\rangle$ and $|\chi_n\rangle$—in other words, the Hamming distance between the image being measured and the original image.

The set of all of the NFCW of a binary image's pixels is referred to as NFCB. Based on that calculated set, the noise density can be estimated, and an optimal noise reduction method can be used based on experimental mapping with the noise density [Pan et al. 2012]. According to a noise judging criterion, each pixel of the image will be discriminated as either "noise" or "pixel." The noise judging criterion differs depending on the noise intensity, the parameters λ_n, and the chosen threshold. The authors compared this proposed method to the classical MF. The conclusion is that their algorithm produces a slightly better PSNR. For a noise intensity of 10%, the method proposed by Pan et al. [2012] produces an image with a PSNR of approximately 15dB, whereas the image filtered by MF has a PSNR of approximately 13%. Therefore, this method requires enhancements in terms of deeper NFCW mining and a better choice of a noise judging criterion [Pan et al. 2012].

Another technique for denoising binary images using a quantum multilayer self-organizing neural network (QMLSONN) was presented in Bhattacharyya et al. [2014]. The proposed method was similar to its classical counterpart, the multilayer self-organizing neural network (MLSONN), in the sense that it worked with three processing layers: input, hiding, and output layers [Bhattacharyya et al. 2014]. These layers contain qubit-based neurons, and that is what made it different from the classical MLSONN. It was used to wipe out uniform Gaussian noise, and it outperforms MLSONN in terms of computational complexity [Bhattacharyya et al. 2014]. For a real-life image, it takes QMLSONN 1.985 seconds to denoise it, whereas it takes MLSONN 5.043 seconds to accomplish denoising. This makes QMLSONN more efficient for real-time applications. Nonetheless, it has not been tested on color images, and that is an important future direction for this field [Bhattacharyya et al. 2014].

From Table II, it can be noticed that the quantum algorithms for image denoising show better results, whether in terms of SNR, PSNR, or MSE. There are still several options that have not been explored in the literature, such as finding a quantum counterpart for the Wiener filter and other classical filters. Hence, there are opportunities to achieve bigger improvements.

5. QUANTUM EDGE DETECTION

Image processing consists of operations necessary for machine vision applications, such as image segmentation, image matching, visual tracking, and image retrieval [Caraiman and Manta 2014, 2015; Benatchba et al. 2006; Youssry et al. 2015]. The foundation of these operations is edge detection [Dubey et al. 2014; Zhang et al. 2012]. Edges define the boundaries of an image [Yuan et al. 2013]. In addition, an edge in images means that a very sharp change in illumination has occurred [Dubey et al. 2014]. In other words, an edge represents the discontinuities in grey-level intensities of an image. According to Ghosh [2013], this can happen for various reasons that include the following:

—Surface normal discontinuity
—Depth discontinuity
—Surface color discontinuity
—Illumination discontinuity.

The basis of edge detection is built on the fact that this discontinuity can be measured by mathematically modeling the variations of intensity across the image and representing them as an equation, and then taking the first derivative of that equation. The maximum value of the first derivative indicates that a change has occurred [Ghosh 2013], and hence there exists a discontinuity. In addition, the gradient can give an indication about the direction and strength of the discontinuity. The direction is given by

$$\theta = \tan^{-1}\left(\frac{\partial f}{\partial y}\Big/\frac{\partial f}{\partial x}\right), \tag{46}$$

and the strength (magnitude) is given by

$$\|\nabla f\| = \sqrt{\left(\frac{\partial f}{\partial x}\right)^2 + \left(\frac{\partial f}{\partial y}\right)^2}. \tag{47}$$

The most frequently used classical methods for edge detection are Sobel's method [Ghosh 2013; Anandakrishnan and Baboo 2014], Prewitt's method [Ghosh 2013; Anandakrishnan and Baboo 2014], and Robert's method [Ghosh 2013; Anandakrishnan and Baboo 2014], which are known as gradient filters. Additionally, the Laplacian of Gaussian (LoG) method [Ghosh 2013; Anandakrishnan and Baboo 2014], which is a type of zero crossing filtering, and Canny's method [Canny 1985] are frequently used as well.

The Canny edge detector operates through the following steps:

(1) Smoothing an image with a Gaussian filter to reduce the noise.
(2) Computing the gradient with its direction and magnitude.
(3) Defining a threshold MT such that

$$M_T(m,n) = \begin{cases} M(m,n) & \text{if } M(m,n) > T; \\ 0 & \text{otherwise.} \end{cases}$$

(4) Using nonmaxima suppression, where the pixels that are not part of the local maximum are set to zero. This makes the edge ridges appear thin. There are two

different thresholds used to do this: t_1 and t_2. Hence, two images are obtained: T_1 and T_2. T_2 has less noise but more false edges compared to T_1.

(5) Finally, the edge segments in T_2 are linked by tracing each segment until its end and then checking its neighbors in T_1 to fill the gaps.

Another method that uses Gaussian filtering is LoG. This method has a smoothing effect caused by convolution with a Gaussian function [Juneja and Sandhu 2009], and its purpose is to reduce the sensitivity toward noise. A Laplacian operator is applied, which can distinguish the grey levels of the image's pixels [Juneja and Sandhu 2009]. The zero crossing pixels are considered as edges [Anandakrishnan and Baboo 2014].

One of the most popularly used edge detection methods due to its easiness is Sobel's method [Senthilkumaran and Rajesh 2009; Anandakrishnan and Baboo 2014; Juneja and Sandhu 2009]. Mathematically, it approximately computes the gradient of the image intensity function using a discrete differentiation operation [Ghosh 2013]. It has two operators, which consist of vertical and horizontal 3×3 masks, as shown in Equation (48). Both masks work as first-order derivatives. The vertical mask (G_y) makes the vertical edges more prominent, whereas the horizontal mask (G_x) makes the horizontal edges more prominent. These masks can achieve that by calculating the differences between the pixel intensities in an edge region and "giving the direction of the largest possible increase from light to dark at the rate of change in that direction" [Ghosh 2013]. This serves to show the severity of changes at a particular point.

$$G_x = \begin{bmatrix} -1 & 0 & 1 \\ -2 & 0 & 2 \\ -1 & 0 & -1 \end{bmatrix} \quad G_y = \begin{bmatrix} 1 & 2 & 1 \\ 0 & 0 & 0 \\ -1 & -2 & -1 \end{bmatrix} \tag{48}$$

Sobel's operator has been extended to the quantum domain in Yi et al. [2014]. The aim was to tackle the real-time limitation of edge extraction algorithms. According to Yi et al. [2014], this limitation can be overcome by finding a quantum equivalent to Sobel's operator, which can be done by combining it with FRQI (discussed in Section 3), resulting in QSobel. Since FRQI uses quantum superposition to represent the image's pixels, QSobel can provide parallel computation and the gradient of these pixels can be evaluated simultaneously [Yi et al. 2014]. This results in exponential speedup and real-time processing. The performance of this operator was compared to the performance of the classical Sobel and Canny. The computational complexity of edge extraction for QSobel with an FRQI image presented by $2^n \times 2^n$ pixels turns out to be $O(n^2)$, whereas for Sobel and Canny the computational complexity is $O(2^{2n})$ [Yi et al. 2014].

Furthermore, Robert's method [Senthilkumaran and Rajesh 2009; Anandakrishnan and Baboo 2014; Juneja and Sandhu 2009] uses a cross operator that is similar to that of Sobel. The regions of high spatial frequencies often correspond to edges. Robert's operator takes advantage of that by making these regions more prominent using a two-dimensional spatial gradient measurement. It uses 2×2 vertical (G_y) and horizontal (G_x) operators, with one of the masks related 90° compared to the other. These operators are shown in Equation (49).

$$G_x = \begin{bmatrix} 1 & 0 \\ 0 & -1 \end{bmatrix} \quad G_y = \begin{bmatrix} 0 & 1 \\ -1 & 0 \end{bmatrix} \tag{49}$$

Prewitt's operator [Senthilkumaran and Rajesh 2009; Anandakrishnan and Baboo 2014; Juneja and Sandhu 2009; Ghosh 2013] is based on the principle of difference of averages, which will reduce the blurriness of the edges while still retaining some smoothing power. This is done by averaging only in the direction along the edge [Ghosh 2013]. The Prewitt operator works on the vertical (G_y) and horizontal (G_x) directions,

as shown in Equation (50).

$$G_x = \begin{bmatrix} -1 & 0 & 1 \\ -1 & 0 & 1 \\ -1 & 0 & 1 \end{bmatrix} \quad G_y = \begin{bmatrix} 1 & 1 & 1 \\ 0 & 0 & 0 \\ -1 & -1 & -1 \end{bmatrix} \tag{50}$$

Dubey et al. [2014] attempted to extend Prewitt's operator to the quantum domain. Whereas the classical Prewitt algorithm uses gradient, the proposed quantum Prewitt's operation modifies the operating bits, which are used as a quantum superposition to give better edge continuity [Dubey et al. 2014]. The authors also claim that their algorithm gives a better quality than any other classical algorithm, such as the Sobel, Canny, LoG, Robert, and Prewitt algorithms.

Other more sophisticated classical edge detection methods exist, such as the differential-based edge detection algorithm, clustering-based edge detection algorithm, and multiscale edge detection algorithm [Zhang et al. 2012]. Each of them has its own advantages and disadvantages, and no single edge detection algorithm that can determine all types of edges has been found yet [Zhang et al. 2012]. Generally, these algorithms are usually used in collaboration with optimization methods, such as ant colony optimization (ACO) [Zhang et al. 2012].

ACO is an optimization method that relies on the concept of pheromones, which ants use to mark the preferred way from a food source to their nests [Zhang et al. 2012]. Ants can smell the pheromone and will choose the path that has a higher pheromone concentration. A similar principle can be used to track the edges of an image and enhance edge detection in terms of quality and performance. However, one of its drawbacks is its computational complexity [Zhang et al. 2012]. An attempt to solve this problem by exploiting the quantum principles of superposition, entanglement, and interference was proposed by Zhang et al. [2012]. The authors proposed quantum ant colony optimization (QACO), where the image's pixels are represented as qubits and the pheromone is updated using quantum rotation gate. They compared their work to that of Nezambadi-Pour et al. [2006], which is one of the methods that uses ACO. For a 128×128 image, their method required 126.9 seconds, whereas QACO required 13.1 seconds, which is 10 times less—a remarkable difference.

Another optimization method used with image processing is emergent computing, which is based on three principles: parallelism, simplicity, and locality [Meshoul and Hussaini 2009]. The principle of emergence is to build something complex by a large group of basic individuals using simple rules. This particular principle is called *reverse emergence*. More details can be found in Meshoul and Hussaini [2009]. The problem with emergence is figuring out which rules can produce the desired complex behavior. This process may take years if it is performed using trial and error. It may also be performed using evolutionary algorithms (EAs), but it still takes large time complexity. Therefore, Meshoul and Hussaini [2009] proposed combining EAs in quantum computing to optimize image processing methods, including edge detection, segmentation, and denoising. The computational complexity has not been reported; however, according to the authors, the proposed method has been tested for image denoising, and the results show effectiveness and robustness [Meshoul and Hussaini 2009]. This research represents a first step toward merging EAs with quantum computing to overcome the computational problems of classical reverse emergence. This is an important step for enhancing edge detection algorithms, as many of them suffer from high computational complexity.

Some of the proposed quantum methods in the literature do not extend any of the classical approaches. For instance, a novel edge detection method was proposed by Yuan

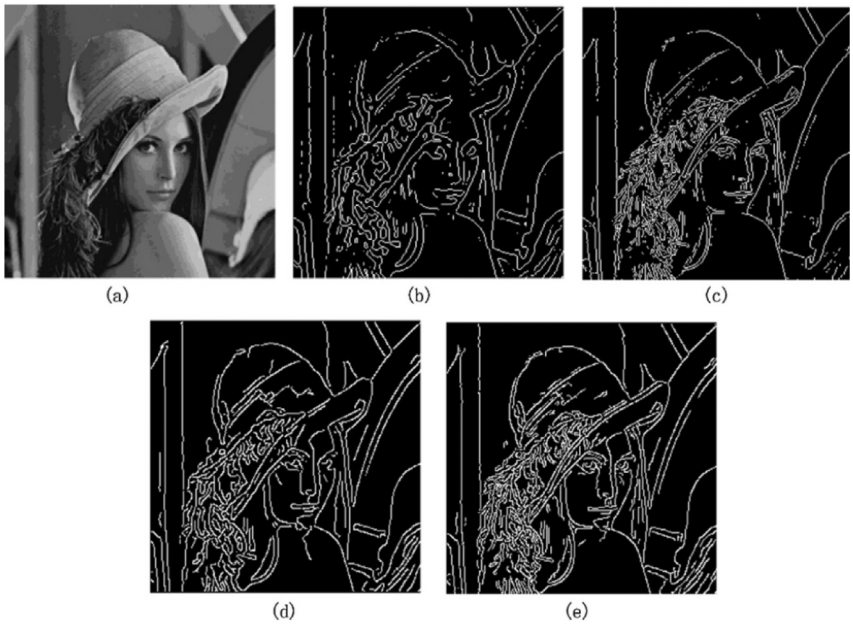

Fig. 10. (a) Original Lena image. (b) Edge detection using the LoG method. (c) Edge detection using Sobel's method. (d) Edge detection using Canny's method. (e) Edge detection using the method proposed by Yuan et al. [2013]. In (b), (c), and (d), there are false edges and some missing edges; (e) shows better details, especially around the eyes.

et al. [2013], where each pixel is represented using a qubit as the following equation:

$$|q(m,n)\rangle = c_0\,|0\rangle + c_1\,|1\rangle. \tag{51}$$

Here, $|c_0|^2$ and $|c_1|^2$ represent the probabilities of getting the states $|0\rangle$ and $|1\rangle$, respectively. The image was smoothed using a Gaussian filter. Then, the row derivative of the Gaussian filter was used as a filter mask. Matrix $a_x(m,n)$ is the output obtained after filtering the image using the filter mask, and matrix $a_y(m,n)$ is the output obtained after filtering the image using the transpose of the filter mask. Finally, the gradient magnitude of each pixel is obtained by the following equation:

$$mag(m,n) = \left[a_x(m,n) + a_y(m,n)\right]^2, \tag{52}$$

which is then normalized into the range [0, 1]. Thus far, the algorithm determines the edge points, gives rise to ridges, and sets all pixels that are not on the ridge top to zeros. The probabilities of $|c_0|^2$ and $|c_1|^2$ are then determined as follows:

$$|c_1|^2 = f(mag(s)), \tag{53}$$

$$|c_0|^2 = 1 - f(mag(s)), \tag{54}$$

where the function f is defined as

$$f(x) = 1/(1 + e^{-(x-a)/b}). \tag{55}$$

The proposed values of a and b in this method are 0.1 and 100, respectively. The authors compared their algorithm to other well-known classical algorithms, such as the LoG method, Sobel's method, and Canny's method, and better output than that with classical ones was reported. Figure 10 shows the output comparison. It can be

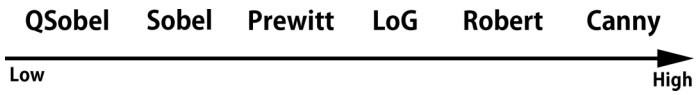

Fig. 11. Order of computational complexity of edge detection methods. QSobel provides the best performance for the lowest computational complexity.

noticed that the method proposed by Yuan et al. [2013] has fewer false edges and better detail in some areas, such as the details of the face and around the eyes.

According to a study conducted by Katiyar and Arun [2014], Canny's method outperforms all of the classical methods, but it has a high computational complexity. Since QSobel outperforms Canny's method, it can be argued that QSobel is the fastest edge detection algorithm producing tangible good results up until now [Yi et al. 2014]. Figure 11 summarizes the superiority of each edge detection method's computational complexity.

An interesting edge detection method was developed by Mastriani [2014b], called *quantum Boolean edge detection*. First, the author proposed a criterion called *pole-to-pole axis only* (PAO), which was exclusively based on projections onto a vertical axis of the Bloch sphere shown earlier in Figure 1. This proposed criterion leads to simple quantum-to-classical and classical-to-quantum interfaces, in addition to simpler development of quantum logical operations. Since only the projections on the vertical axis need to be measured, the author argued that this interface was optimal and more robust. The goal behind developing this criterion is to make the extension of classical algorithms to the quantum domain easier. First, the author proposed a classical Boolean edge detection. The algorithm consists of a kernel that scans the image's pixels. The operation of this kernel consists of three steps. The first step is to apply an OR Boolean operation to the kernel's pixel values, excluding the center pixel. The second step is to perform an XOR Boolean operation between the resultant value from the previous step and the center pixel. Finally, the center pixel is replaced with the result from the XOR Boolean operation. By the logic of the POA criterion, the extension of these steps to the quantum domain becomes straightforward. For more details and a full explanation on the derivation of the POA criterion, the reader is referred to the work of Mastriani [2014b]. A comparison between the results of the classical and the quantum versions of this algorithm is shown in Figure 12.

Generally, the quantum algorithms for edge detection show computational superiority and precision over the classical ones. Since there is no perfect edge detection algorithm that can detect all types of edges, one best way to move forward is to combine several algorithms. The algorithms that need be combined must be robust [Zhang et al. 2012]. Hence, the future of quantum-based edge detection is based in coming up with robust algorithms with better time complexities that can be combined with other algorithms for better detection.

6. IMAGE UNDERSTANDING AND COMPUTER VISION

Computer vision and image understanding are closely related areas to image processing, as it requires preprocessing using image processing. However, since computer vision by itself is a very broad area of research, only the major contributions in QuIP related to this field will be discussed in this article.

Local feature extraction is one of the important artificial intelligence tasks that is utilized in image processing for computer vision applications and for enhancing image understanding. This method lacks a quantum counterpart, which leads to a limitation to quantum image understanding, according to Zhang et al. [2015]. Therefore, in their work, an attempt is made to apply local feature extraction on quantum computers through a quantum feature extraction framework based on NEQR. This particular

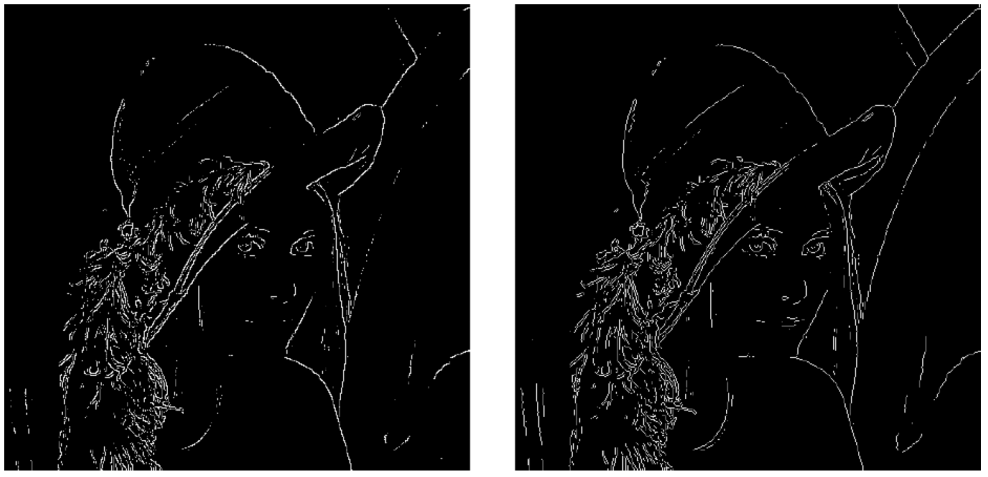

Fig. 12. Result of classical Boolean edge detection (a) and the result of the quantum Boolean edge detection (b) [Mastriani 2014b]. The latter shows more details, and the lines appear less dotted.

image representation model is used because the color information from the pixels are stored in the basis states of a qubit sequence. Hence, quantum image addition and subtraction can be performed flexibly. In addition, the gradient of the image's pixels can be computed for all of them simultaneously due to quantum superposition and parallelism. The features can then be extracted via a gradient threshold. Zhang et al. [2015] reported a complexity of $O(n^2 + q^2)$ for greyscale images of size $2^m \times 2^n$ and a grey range of $[0, 2^q - 1]$, where m and n are entangled qubits, and q is the length of the qubit sequence required to store the greyscale of pixels.

An important aspect of image understanding in computer vision involves searching and similarity matching. The first work in this field was carried out by Yan et al. [2012]. The similarities between two images of the same size represented by FRQI was estimated on the basis of the probability distribution of the results from quantum measurements. Although the algorithm is fast, its complexity is proportional to the size of the image. In addition, the result of similarity matching depends on the information in the entire image. FRQI has also been used as a fundamental representation for designing a binary image search algorithm based on probability distributions in Yan et al. [2012]. Twelve qubits are used to encode the images, and seven quantum measurements are performed to get the probability distributions. The experiments show that this method requires fewer computational resources compared to classical search algorithms. In Zhou and Sun [2015], a similarity comparison algorithm was developed based on NAQSS representation to prove the feasibility and effectiveness of these operations on quantum computers. Experiments showed that indeed these operations are feasible on quantum computers, and this is a step toward enlarging and developing more complex operations.

Image morphology assists in understanding the image and analyzing it. Some preliminary work in quantum image morphology was presented in Yuan et al. [2014a]. The feasibility of two types of morphology were tested on quantum images represented by NEQR, which include quantum binary and greyscale morphological operations. Quantum circuits for dilation and erosion were designed. In this algorithm, quantum parallelism and Grover's search algorithm were well utilized. According to the time analysis, the complexity of this algorithm could be lower than or equal to its classical

counterpart. In Zhou et al. [2015b], dilation and erosion have been extended to the quantum domain by using the quantum loading scheme (QLS), which is a "unitary operation that loads all information of data set into quantum state from electronic memory" [Chao-Yang 2007], and Boyer's algorithm [Chao-Yang 1996]. The algorithm presented time complexity much smaller than classical morphology.

Other accomplishments within quantum application in computer vision include the Quantum RANSAC algorithm [Caraiman and Manta 2009], which is used for model fitting and is essential to computer graphics and vision in general. All of the discussed quantum geometric transforms can be considered as an initiative to study more complicated transforms. Furthermore, according to Caraiman and Manta [2012], quantum solutions have been derived for essential different problems, and there is no complete pipeline for full image rendering on quantum computers as of yet. Nonetheless, these solutions could also be useful in other applications, such as image watermarking and cryptography, which are explored more in Section 8.

7. IMAGE TRANSFORMATIONS

Image transformations are important for image analysis, and it is used in many applications, including those in image understanding and computer vision as discussed in the previous section. An example of such an application is in motion correctness. The first step of motion correctness is image registration, which involves transforming the image by resampling it according to parameters determined by a reference image. Therefore, image transformations, such as image scaling, translation, and geometric transformations, are widely studied on classical computers [Sonka et al. 1993]. However, it has not been sufficiently studied on quantum computers, which makes it a fertile area for research.

Image scaling utilizes interpolation, which is the process of estimating the values at unknown locations using the values at known locations. The first attempt to achieve image scaling on quantum computers was conducted by Jiang and Wang [2015]. First, the method proposes to improve on NEQR in a way that allows storing images of size $2^{n1} \times 2^{n2}$ instead of square images only. Second, interpolation using nearest neighbor is extended to the quantum domain. Although this interpolation method produces a poorer quality compared to bilinear and bicubic methods, it is simple and easy to realize. Therefore, it represents an initial step toward extending the research of image scaling on quantum computers.

Another important image transformation is translation. This translation could be either entire translation (ET), which moves the whole image, or cyclic translation (CT), which is often used as an intermediate step in image processing, such as shifting the zero frequency component to the center of the image's spectrum after applying Fourier transformation. Both types of image translation do not have any extensions in quantum computers using quantum adders and comparators. The first approach toward extending image translation to quantum computers was attempted by Wang et al. [2015a]. The proposed algorithm is based on NEQR and can be applied to $2^n \times 2^n$ greyscale images. The translations in the left and right directions are processed differently, which causes the complexity of the network circuit to increase. Therefore, one future direction could focus on reducing the complexity of the network. In addition, it could also be possible to consider studying partial translations.

Strategies for designing geometric transformations were discussed in the work by Le et al. [2011c]. The goal of such research is to focus on the image's areas that are affected by the transformation, smoothness, and separability, which can be exploited by representing images on quantum computers extensively. Here, the algorithms are based on FRQI for all images to be able to effectively encode the essential information about the image, such as color and position. Despite initial progress, Le et al. [2011c]

consider this as a start toward improving these algorithms for more flexible applications. In addition, producing circuits with lower complexities is also considered as a future improvement.

Geometric transformation is an essential step for many tasks, including encryption, and it is especially important for image registration. Some examples include resizing, rotating, and cropping. The first attempt to extend these operations to quantum computers was published by Le et al. [2010]. The method proposed in their work extended geometric operations that are applied to N-size images, such as two-point swapping, flip, coordinate swapping, and orthogonal rotations to the quantum domain by using basic quantum gates that include NOT, CNOT, and Toffoli gates. The simulation of these quantum operations lead to complexities of $O(log^2 N)$ for the first operation and $O(logN)$ for the rest. In classical geometric transforms, global operations are generally slower than local ones. However, the opposite is true for its quantum counterparts. Nonetheless, these problems might have been caused due to unavoidable memory and space problems when simulating the operations on a classical computer. The complexities discussed for the aforementioned quantum image transformation algorithms are listed in Table III.

8. QUANTUM IMAGE SECURITY

Information hiding and security are popular topics in computing and communication, especially in systems where privacy and security are crucial requirements. The data transmitted through communication lines can be in the form of multimedia, particularly images and videos. Some of the popularly used methods for securing such transmitted visual signals include cryptography, steganography, and watermarking [Cox et al. 2008; Zhang et al. 2013b; Yang et al. 2013a]. The aim of visual cryptography is to transform the image into an unidentifiable form to protect it during transmission [Song et al. 2013]. On the other hand, the aim of steganography is to hide the existence of the message by "embedding symbolic information into public data" [Cox et al. 2008; Zhang et al. 2013b; Song et al. 2013]. One type of steganography is image scrambling. Although many consider that there exists an overlap between the fields of watermarking and steganography, they are different. Watermarking is concerned with embedding information in the carrier signal that would help to identify its real owner, and the watermarking signal could be either visible or invisible.

Moving on to the issue of security from a quantum computing perspective, it was earlier mentioned in Section 1 that quantum computers can break integer factorization and elliptic curve–based cryptography. Here, the impact of quantum computers on security can be mitigated by the appropriate use of certain principles of quantum physics. For example, using the uncertainty inherit in the measurement of a quantum object, encryption protocols can be designed in such a way that they provide unconditional detection of intrusion, and therefore unconditional security against quantum computer attacks. QKD is the area of security that studies such quantum security protocols [Bennett and Brassard 2014; Branciard et al. 2005; Ekert 1991].

In the next sections, QuIP will be explored from a security perspective, which includes encryption, watermarking, and scrambling. Although these three categories can be studied separately, they might overlap in some cases, such as some encryption scheme used in watermarking or scrambling.

8.1. Encryption

Cryptography means encrypting data using an encryption key and then sending the resulting encrypted data through communication channels, which can be decrypted at the receiver's end using a decryption key [Harris 2012]. The goal is to secure data across communication lines and make the data being sent and received accessible only

by the authorized parties who have these keys. If the encryption and decryption keys are the same, then the cryptography algorithm is known as symmetrical. Otherwise, it is known as asymmetrical. In asymmetric cryptography, the sender encrypts the data using a public key, and the receiver decrypts it using a private key that no other entity can have access to [Harris 2012]. On the other hand, the keys used for encryption and decryption in symmetric cryptography are shared between the sender and the receiver, and they are either exactly the same or can be obtained using a simple conversion operation. This is why asymmetric cryptography is considered more secure than symmetric cryptography [Harris 2012]. Some of the contributions in this field can be found in the following works [Wang et al. 2008; Ding and Jing 2010; Zhu et al. 2010; Kaushik et al. 2014; Zhang and Ding 2015].

An encryption algorithm using QWT was proposed by Wang et al. [2014], which is an extension of the method proposed in Wang et al. [2008]. The authors proposed applying double diffusion to the image after transforming it to the frequency domain using a WT. In addition, a chaotic logistic map was used to ensure the uniformity of the distribution of the image's color information. The authors analyzed their algorithm theoretically and concluded that it is feasible since the operations follow the rules of quantum mechanics. All of the operations are unitary, which means that they are reversible, and hence decryption can be implemented by simply reversing the process.

A different scheme of encryption was proposed by Hua et al. [2015], who developed a quantum encryption algorithm based on correlation decomposition. The basic idea is to correlate the pixels of the image using quantum superposition and quantum measurement. Based on that, the image is divided into subimages, which are represented as a binary tree. The color information in each subimage is encoded using a quantum random-phase operation, quantum revolving operation, and Hadamard transform. Superimposing the subimages produces the encrypted image. The authors analyzed their algorithm theoretically from a security perspective and computational complexity perspective. This analysis concluded that the algorithm was robust against brute-force attack and had a computational complexity of $O(N2^{2n})$, which is lower than its classical counterpart.

In Yang et al. [2013b], an encryption algorithm that generalizes the double-phase random encoding (DPRE) into a quantum equivalent was proposed. DPRE was first proposed by Refregier and Javidi [1995]. The algorithm is used in image security to transform the image that needs to be encrypted into a complex-valued encoded image by applying independent random-phase encoding on both the spatial plane and the Fourier plane [Refregier and Javidi 1995]. In contrast, Yang et al. [2013b] applied a phase encoding operation to a greyscale image in the spatial domain and the frequency domain to enhance the security of the proposed algorithm. All of the operations are unitary, and hence decryption could be applied by reversing the processes. The authors analyzed their algorithm theoretically and concluded that its computational complexity is $O(n^2)$. The computational complexity is reasonably low due to QFT, which is much faster compared to the classical FFT $O(n2^n)$.

Zhou et al. [2012] proposed a quantum image encryption scheme in using geometric transforms. However, Yang et al. [2014] argued that this proposed scheme was invalid because it violated the rules of quantum physics. Therefore, Yang et al. proposed an encryption algorithm for colored images based on QFT with DPRE. The authors analyzed the computational complexity, which turned out to be in the order of $O(n^2)$, as opposed to its classical counterpart, which is $O(n^8)$. Again, this was due to the effect of switching from the classical FFT to the QFT. In addition, the authors performed key sensitivity analysis and robustness analysis, concluding that the algorithm was robust due to the large key space, which made it hard for nonauthorized users to obtain the correct keys for retrieving the original image.

As mentioned previously, geometric transforms are used for image encryption schemes to enhance security. An example for such usage of geometric transforms on quantum computers is demonstrated in Song et al. [2014b]. Restricted geometric transforms were used to shuffle the pixels' positions, then a quantum diffusion operation was implemented based on restricted color transformations. Sensitive chaotic maps were used to generate encryption keys, which further enhanced security. The theoretical analysis proved that the algorithm was secure and robust against eavesdropping attacks.

Other attempts in the literature to encrypt images on quantum computers include an image encryption scheme based on a quantum logistic map, which reported an acceptable speed, large key space, and high security level according to Akhshani et al. [2012]. In addition, the least significant qubit (LSQb) information hiding algorithm [Wang et al. 2015b], which was designed based on NEQR, indicated a high PSNR of 64.973 for a standard Lena image.

Generally, most of these algorithms involve theoretical analysis without implementations or simulations. Therefore, none of them reports any quality metric, such as PSNR and MSE. This is an indication that this area is open for research and has the potential to grow and expand. It is worth mentioning that encryption on quantum computers is now being extended to include videos. An example of such work is mentioned in Yan et al. [2015]. Since encryption can be time consuming for a large number of frames, the goal of the proposed method is to enhance the speed of the encryption and decryption using MCRQI while maintaining security.

8.2. Watermarking

Watermarking is the process of embedding information in a carrier signal, such as an image. It is typically used for authentication, copyright management, and content protection [Potdar et al. 2005]. The sudden increase in the attention toward watermarking emerged due to the importance of copyright protection, especially across the Internet, where the ease of sharing digital content jeopardizes copyrights of the original owner. To ensure that the identity of the original content provider does not get lost, a watermark signal is used. Watermark is a signal that is either visible or invisible, containing information about the copyright owner [Cox et al. 2008]. Therefore, this watermark signal can be regarded as a signature that can be embedded into multimedia, such as images and videos. A general watermark embedding algorithm is shown in Figure 13. According to Potdar et al. [2005], digital watermarking imposes three main requirements for guaranteeing security. The first requirement is robustness, which guarantees the ability to extract a watermark even if it becomes altered through intentional or unintentional attacks. The second requirement is transparency, which means that the watermark can be added without distorting the image or necessitate cropping. Finally, the third requirement is data payload, which is the amount of data that should be embedded to guarantee uniqueness of the signal and the successful extraction of the watermark [Potdar et al. 2005].

The embedding process is decided using a secret key, which determines the locations in the image where the watermark is to be embedded [Potdar et al. 2005]. Using the same key, the embedded watermark can be extracted. It is important to choose a key that satisfies the three requirements mentioned previously. More details and key contributions can be found in these studies [Potdar et al. 2005; Yusof and Khalifa 2007; Chandra et al. 2010; Qianli and Yanhong 2012; Ho et al. 2002; Salama et al. 2011; Tianming and Yanjie 2011; Sridevi and Fatima 2013; Andalibi and Chandler 2015; Maheshwari et al. 2015; Kallianpur et al. 2015].

Investigations within quantum image watermarking began due to the flexibility offered by image representations in the quantum space [Zhang et al. 2013b]. For example,

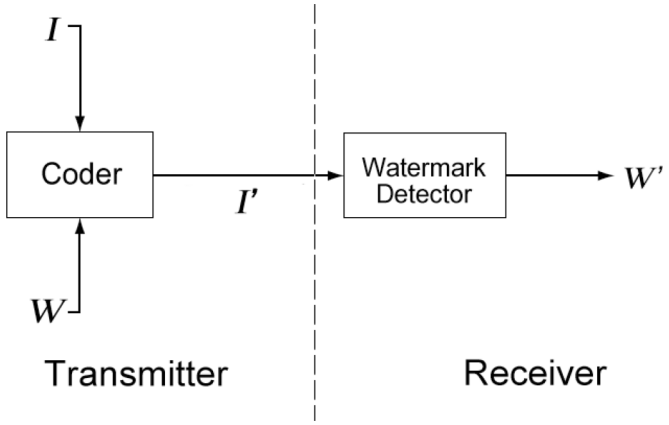

Fig. 13. Generic watermarking scheme [Cox et al. 2008]. In this scheme, I represents the image to be transmitted, W represents the watermark, I' represents the image after embedding the watermark to it, and W' represents the detected watermark after the image arrives on the receiver's side.

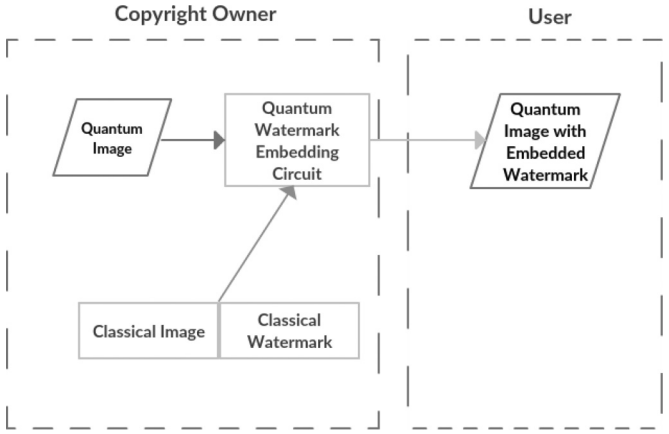

Fig. 14. WaQI procedure [Yan et al. 2014]. The owner of the image has access to both the classical and quantum versions of it, while other users have access to the quantum image only after the watermark has been embedded.

according to Yan et al. [2014], the pioneer strategy of quantum image watermarking is called the watermarking and authentication strategy for images on quantum computers (WaQI). This strategy was built based on FRQI. It is keyless in the sense that it does not rely on secret exchange of encrypted information [Yan et al. 2014]. Instead, it relies on the geometric transformations of the image's contents. The watermark is embedded over two stages. The first stage is to control the access of the various stages of the image; copyright owners have access to both the classical and quantum versions of the image, whereas other users have access only to the quantum version of the image [Yan et al. 2014]. The second one is to embed the watermark in the classical version of the image and then transform it to its quantum version [Yan et al. 2014; Iliyasu 2013; Iliyasu et al. 2012]. These two stages are shown in Figure 14. This watermarking strategy was improved later and a new scheme was proposed, called *the two-tier greyscale version of the WaQI protocol* (GWaQI) [Bun et al. 2013b]. According to Yan et al. [2014], "the purpose of the GWaQI scheme was to implement a bi-level scheme that included embedding a conspicuous watermark logo in a predetermined sub-area of the cover

image; meanwhile, the same watermark signal was embedded to cover the rest of the image in an obscure manner." Therefore, the whole circuit of GWaQI consists of two main sections: one for embedding the visible watermark and the other for embedding the invisible watermark. An illustration of the general realization of GWaQI can be found in Yan et al. [2014].

A similar approach to quantum watermarking based on FRQI was attempted in Zhang et al. [2013a]. The goal of this research was to develop a watermarking strategy that would only enable legal owners to extract the watermark image. The proposed watermark strategy demonstrated its ability to reach to its maximum capacity, which is equal to the size of the carrier image. The algorithm was quantitatively evaluated using PSNR, and a value of 64.8810dB for a standard Lena image was reported.

Yan et al. [2015b] proposed a WaQI based on MCRQI instead of FRQI. Their scheme is based on generating double keys using quantum algorithms and embedding the watermark in both the spatial and frequency domains. According to the authors, this strategy outperformed WaQI, which was based on FRQI. The PSNR of this algorithm reached as high as 43dB for some images. Another extension of WaQI was proposed in Zhang et al. [2013b]. Here, quantum image watermarking using QFT was investigated. The watermark image was processed using a quantum circuit to ensure the security of the watermark image. Further, the watermark was embedded within the Fourier coefficients. QFT was used to ensure that the image would not be cropped or contaminated with noise [Zhang et al. 2013b]. Experimental results showed high PSNR values in the order of 45.3864dB for some images. In an extension to the algorithm described by Zhang et al. [2013b], an improved strategy was proposed by Yang et al. [2013a], in which instead of directly mapping a classical watermarking into its quantum equivalent as in Zhang et al. [2013b], the operations were made to be unitary. Yang et al. [2013a] suggested an improved algorithm, incorporating the QFT as suggested in Zhang et al. [2013b].

In Song et al. [2013], a dynamic quantum watermarking scheme was proposed for securing quantum images using FRQI with QWT. According to this method, the first step was to extract wavelet coefficients from the quantum image. This was accomplished by applying QWT on the image. Further, to control the embedding strength, a dynamic diagonal vector was utilized. This offered better flexibility than the classical schemes, in which the parameter used for the embedding process remained fixed. This dynamic diagonal vector was decided using the carrier and the watermark images, which was assumed to only be known by the authorized owner of the image. Hence, it was used as a key for the extraction process [Song et al. 2013]. The authors used optimized matrices to make sure that the final representation of the image was visually clear. Experimental results depicted a significantly high PSNR value that reached 81.77dB on some images. The proposed scheme had a computational complexity of $O(4n^2)$ in comparison to $O(8^n)$ for its classical counterpart. In an extension, Yang et al. [2014] reviewed and improved the scheme proposed by Song et al. [2013], which suffered similar limitations of Zhang et al. [2013b] in mapping the classical to its equivalent quantum algorithm. As an example, embedding the watermark image into the coefficients could be done using classical algorithms simply by adding grey levels of the watermark image to the coefficients. However, a similar approach cannot be implemented in the quantum domain. Therefore, a theoretical improvement suggested by Yang et al. [2014] involved the use of a phase rotation operation that rotates the original carrier image pixel by the embedded degree, which was decided by the embedded algorithm [Yang et al. 2014].

An adaptive watermarking approach based on weighted quantum particle swarm optimization (WQPSO) was proposed in Soliman et al. [2015]. The authors tested the robustness of their algorithm against JPEG compression, cropping attacks, and various noise attacks. They also compared their algorithm to PSO and QPSO [Sun et al. 2004;

Table III. Comparison Between Image Transformation Schemes

Method	Computational Complexity	Image Size
Jiang and Wang [2015]	—	$2(n1) \times 2(n2)$
Zhang et al. [2015]	$O(n^2 + q^2)$	$2^n \times 2^n$
Wang et al. [2015a]	—	$2^n \times 2^n$
Le et al. [2010]	$O(logN)$	

Table IV. Comparison Between Watermarking Schemes

Method	PSNR (dB)	Computational Complexity
Zhang et al. [2013b]*	45.3864	—
Song et al. [2013]*	81.77	$O\left(4n^2\right)$
Song et al. [2013]	—	$O(8^n)$
PSO [Sun et al. 2004]	54	—
QPSO* [Sun et al. 2004]	54	—
WQPSO* [Soliman et al. 2015]	55	—
Song et al. [2014a]*	80.09	$O(n)$
Hua et al. [2015]*	—	$O\left(N2^{2n}\right)$
Yang et al. [2013b]*	—	$O\left(n^2\right)$
Yang et al. [2014]*	—	$O\left(n^2\right)$
Jiang et al. [2014b]*	—	$O(n)$

*Denotes a quantum method.

Soliman et al. 2015], and it illustrated a better PSNR that reached approximately 55dB, whereas in comparison the other two methods reached 54dB [Soliman et al. 2015]. However, the weighted coefficients in the algorithm were updated linearly. The authors believed that enhancing the adaptability of the algorithm could lead to better performance [Soliman et al. 2015].

A dynamic watermarking scheme based on FRQI and Hadamard transform was proposed in Song et al. [2014a]. As in the previous algorithms, this proposed scheme utilized a dynamic matrix to control the embedding process rather than the fixed parameters that were used in other classical schemes. The PSNR reached up to 80.09dB for some of the processed images, at a computational complexity of $O(n)$ [Song et al. 2014a].

A comparison between all discussed methods are summarized in Table IV. The method proposed by Song et al. [2014a] demonstrates the best computational complexity at a very high PSNR when compared to other algorithms. Although the method proposed by Song et al. [2013] has a slightly higher PSNR in comparison to Song et al. [2014a], its computational complexity is not linear, which provides Song et al. [2014a] a major advantage. The future of quantum image watermarking may require obtaining a reasonable trade-off between improvements in PSNR without the compromise in computational complexity.

8.3. Scrambling

Image scrambling is a method that is used as a preprocessing or postprocessing step [Jiang et al. 2014b] in image security. The main purpose of image scrambling is to disorder the form of the image to enhance its security. It has two categories: changing the pixel position and changing the pixel value [Zhou et al. 2015c]. Some examples of the first category include Hilbert transform [Hu et al. 2010], Arnold transform [Bing and Jia-Wei 2005], and Fibonacci transform [Mishra et al. 2012; Zhou et al. 2015c]. The main algorithms for the second category are grey transform [Zou and Ward 2003], “or” transform [Ravankar and Sedukhin 2011], and bit-plane transform [Lie and Ping Tian 2011].

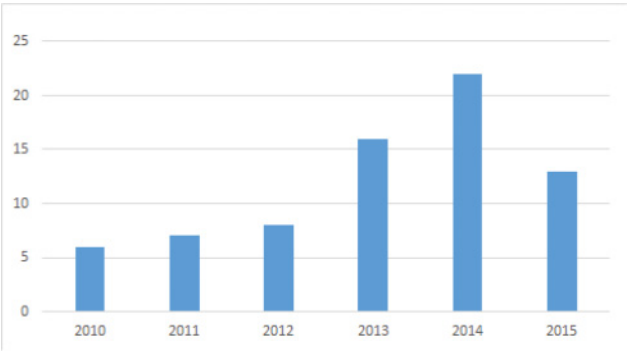

Fig. 15. Bar chart of the number of QuIP works published between 2010 and 2015. The number of works has been increasing, which indicates that the field of QuIP is getting more attention.

An attempt to extend Arnold and Fibonacci transforms to the quantum domain was proposed in Jiang et al. [2014b]. The proposed algorithm was based on FRQI, and it used a plain adder and adder module N to factor the classical operations into unitary operations using controlled-not and Toffoli gates. The theoretical analysis of this framework showed that the proposed algorithm had a linear complexity. A similar work was also carried out in Jiang et al. [2014a], where an extension to Hilbert image scrambling to the quantum domain was proposed. This algorithm resulted in a linear complexity.

The first attempt in the literature to extend the second category of image scrambling to the quantum domain was proposed in Zhou et al. [2015c], in which the authors argued that for the first category, the cost of the circuits becomes high as the size of the image increases, whereas their scheme limited the size of the image being scrambled to $n \times n$.

The field of quantum image scrambling is mostly limited to theoretical analysis without in-depth implementation or practical evaluations. Therefore, very limited evidence is available to prove the effectiveness of such approaches using qualitative or quantitative metrics, which makes it challenging for comparison and benchmarking.

9. STATISTICS AND TRENDS

This survey has presented a review of more than 70 works that encapsulate both classical and quantum methods in image processing. A large majority of these works were acquired through a simple search of relevant publications in the area within individual digital libraries, such as the IEEE, Elsevier, and Springer. The advances and trends in QuIP algorithm development have been drawn in the context of classical and QuIP studies published between 2010 and 2015. From Figure 15, it can be noticed that the attention around QuIP has been an increasing trend, with a particularly sharp increase in 2014. Despite the shortfall in 2015, the number of studies in 2015 has surpassed the number compared to years prior to 2013. Furthermore, leading journals have been giving more attention to QuIP. The issue published in Venegas-Andraca [2015] can be taken as a good example.

In line with the organization of this article, most of the surveyed QuIP publications were classified into into one of the following broad categories: image storage, retrieval, and compression; image denoising; image edge detection; image understanding and computer vision; image transformations; and image security. Figure 16 shows the total percentage of research work in QuIP conducted within each category. It can be noticed in the figure that quantum image security has been receiving the most attention,

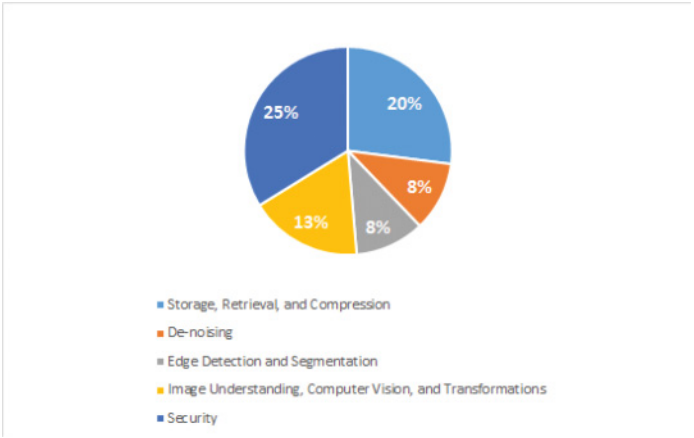

Fig. 16. Pie chart showing the percentage of publications in each category. Edge detection has the lowest percentage, which means that this area requires more research focus.

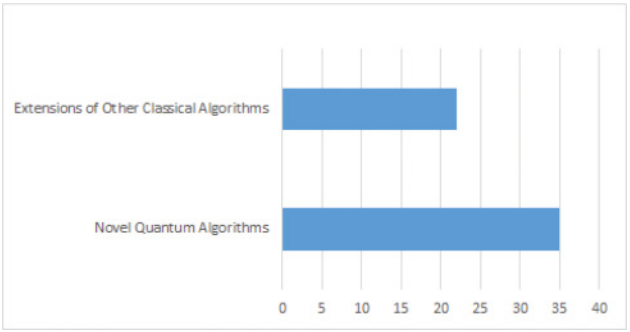

Fig. 17. Bar chart showing the number of novel quantum methods and the number of quantum methods that extend existing classical methods for each imaging category. The number of novel quantum algorithms built from scratch exceeds the number of extended classical ones.

followed by quantum storage, retrieval, and compression. This trend could be due to the secure nature of quantum mechanics, as this was one of the initial motives to incorporate it into classical computers, aside from the fact that it is expected to increase computational performance. The category that has the least percentage is edge detection, indicating the need for further research to focus on the challenges of image segmentation. As mentioned earlier, good edge detection techniques are crucial for bridging the gap between image understanding and computer vision.

Generally, QuIP algorithms can be developed from scratch from novel ideas or can be an extended quantum equivalent of already-existing classical algorithms. In Figure 17, a statistical summary of the literature in QuIP based on the aforementioned classification is illustrated. It can be noticed that the number of QuIP algorithms that directly extend their classical counterpart is much less than the number of the ones built from scratch. In addition to possibly concluding that it is often easier to build newer quantum methods from novel ideas than extend classical counterparts, it is also important to note that a direct mapping of classical theories into the quantum domain is not often feasible, as quantum operations must be invertible and unitary (as discussed in Section 8.2). An example of such cases includes the convolution and correlation operators [Lomont 2003; Caraiman and Manta 2013].

Finally, it is also worth noting that 65% of the algorithms in the QuIP works surveyed rely on FRQI representation as a basis to their model. In addition, 3% of the works dealt with binary images, whereas 29% dealt with greyscale images and the other 58% targeted colored images.

10. CONCLUSION

In this article, the application of quantum information models to image storage, retrieval, compression, denoising, edge detection, and watermarking have been reviewed. In addition to the detailed study of such QuIP algorithms in the literature, quantitative and qualitative comparisons presented between the classical and corresponding quantum counterparts have supported the conclusion that quantum algorithms prevail over classical ones both in terms of performance and computational complexity. With the growing trends in quantum computing, it can only be anticipated that visual information processing in the quantum domain can produce a deep impact in enhancing machine vision for real-time applications. Further, research has also revealed that the transitioning between the classical and quantum domains for image processing needs is not complicated as long as the underlying principles of quantum mechanics, such as maintaining the circuits unitary and invertible, are followed.

Despite much research attention in recent years, several limiting factors regarding the development of QuIP could be also noted. First, the reliance on certain functionally basic algorithms has often stalled further improvements in them. For example, several recently developed QuIP algorithms have considered FRQI as their basis without further exploring improvements on it. Second, much like in other fields, the evaluation of QuIP algorithms has been based on visual quality, which is often subjective, and on quantitative metrics such as SNR, PSNR, MSE, and computational complexity. It is generally recommended to have standard, consistent, and reliable evaluation protocols that will facilitate appropriate benchmarking of both current and future developments in QuIP algorithms.

A statistical summary of the literature in QuIP was also reported in this article. According to this summary, it could be noticed that there is a growing need to focus research on specific areas within QuIP, such as in quantum image edge detection, which when pipelined with image segmentation can hugely impact several high-level computer vision tasks. For example, the research conducted by Talbi et al. [2007] indicates that quantum image segmentation shows more promising results than its classical counterpart. However, to improve this further, quantum image edge detection needs to be improved first.

Finally, this survey briefly overviewed some of the potential opportunities that shall allow for greater development and improvement in the field of QuIP to enable future research in this domain. With the rapid developments in computational methods for visual signal processing, it is anticipated that continuous growth in QuIP will provide the opportunity for processing visual big data in a meaningful, efficient, and effective manner.

REFERENCES

N. Ahmed, T. Natarajan, and K. R. Rao. 1974. Discrete cosine transform. *IEEE Transactions on Computers* 23, 1, 90–93.

A. Akhshani, A. Akhavan, S.-C. Lim, and Z. Hassan. 2012. An image encryption scheme based on quantum logistic map. *Communications in Nonlinear Science and Numerical Simulation* 17, 12, 4653–4661.

N. Anandakrishnan and S. Santhosh Baboo. 2014. An evaluation of popular edge detection techniques in digital image processing. In *Proceedings of the International Conference on Intelligent Computing Applications (ICICA'14)*. 213–217.

Mehran Andalibi and Damon M. Chandler. 2015. Digital image watermarking via adaptive logo texturization. *IEEE Transactions on Image Processing* 24, 12, 5060–5073.

John C. Baez. 2004. Quantum Quandaries: a Category-Theoretic Perspective. Retrieved December 9, 2016, from http://math.ucr.edu/home/baez/quantum/quantum.html.

Glenn Beach, Chris Lomont, and Charles Cohen. 2003. Quantum image processing (QuIP). In *Proceedings of the 32nd Applied Imagery Pattern Recognition Workshop*. 39–44.

Karima Benatchba, Mouloud Koudil, Yacine Boukir, and Nadjib Benkhelat. 2006. Image segmentation using quantum genetic algorithms. In *Proceedings of the 32nd IEEE Annual Conference on Industrial Electronics (IECON'06)*. 3556–3563.

Charles H. Bennett and Gilles Brassard. 2014. Quantum cryptography: Public key distribution and coin tossing. *Theoretical Computer Science* 560, 1, 175–179.

Charles H. Bennett, Gilles Brassard, Claude Crépeau, Richard Jozsa, Asher Peres, and William K. Wootters. 1993. Teleporting an unknown quantum state via dual classical and Einstein-Podolsky-Rosen channels. *Physical Review Letters* 7070, 1895–1899.

Siddhartha Bhattacharyya, Pankaj Pal, and Sandip Bhowmick. 2014. Binary image denoising using a quantum multilayer self organizing neural network. *Journal of Applied Soft Computing* 24, 717–729.

Li Bing and Xu Jia-Wei. 2005. Period of Arnold transformation and its application in image scrambling. *Journal of Central South University of Technology* 12, 1, 278–282.

Niels Bohr. 1913. On the constitution of atoms and molecules. *Philosophical Magazine* 26, 1, 1–25.

Max Born. 1926. Quantenmechanik der stovorgange. *Zeitschrift für Physik* 38, 803–827.

Luis J. Boya. 2004. The thermal radiation formula of Planck (1900). arXiv:0402064.

Cyril Branciard, Nicolas Gisin, Barbara Kraus, and Valerio Scarani. 2005. Security of two quantum cryptography protocols using the same four qubit states. *Physical Review A* 72, 3, 032301.

G. Brida, M. Genovese, E. Monticone, C. Portesi, M. Rajteri, and I. Ruo-Berchera. 2010. Experimental sub-shot noise quantum imaging versus differential classical imaging. In *Proceedings of the 4th IEEE International Conference on Quantum, Nano and Micro Technologies*. 71–76.

Antoni Buades. 2005. A non-local algorithm for image denoising. In *Proceedings of the IEEE Computer Society Conference on Computer Vision and Pattern Recognition (CVPR'05)*. 60–65.

John Canny. 1985. A computational approach to edge detection. *IEEE Transactions on Pattern Analysis and Machine Intelligence* 8, 6, 679–698.

Simona Caraiman and Vasile I. Manta. 2009. New applications of quantum algorithms to computer graphics: The quantum random sample consensus algorithm. In *Proceedings of the 6th ACM Conference on Computing Frontiers*. 81–88.

Simona Caraiman and Vasile Manta. 2012. Image processing using quantum computing. In *Proceedings of the 16th International Conference on System Theory, Control, and Computing (ICSTCC'12)*. 1–6.

Simona Caraiman and Vasile I. Manta. 2013. Quantum image filtering in the frequency domain. *Advances in Electrical and Computer Engineering* 13, 3, 77–84.

Simona Caraiman and Vasile I. Manta. 2014. Histogram-based segmentation of quantum images. *Theoretical Computer Science* 529, 46–60.

Simona Caraiman and Vasile I. Manta. 2015. Image segmentation on a quantum computer. *Quantum Information Processing* 14, 5, 1693–1715.

Munesh Chandra, Shikha Pandel, and Rama Chaudharl. 2010. Digital watermarking technique for protecting digital images. In *Proceedings of the 3rd IEEE International Conference on Computer Science and Information Technology (ICCSIT'10)*. 226–233.

Pang Chao-Yang. 1996. Tight bounds on quantum searching. *Fortschritte der Physik* 46, 493–506.

Pang Chao-Yang. 2007. Loading N-dimensional vector into quantum registers from classical memory with O(logN) steps. arXiv:0612061.

W.-H. Chen and W. K. Pratt. 1984. Scene adaptive coder. *IEEE Transactions on Communications* 32, 3, 225–232.

Ingemar J. Cox, Matthew L. Miller, Jeffery A. Bloom, Jessica Fridrich, and Ton Kalker. 2008. *Digital Watermarking and Steganography* (2nd. ed.). Elsevier.

David Deutsch. 1985. Quantum theory, the Church-Turing principle and the universal quantum computer. *Proceedings of the Royal Society of London* 400, 1818, 97–117.

David Deutsch and Richard Jozsa. 1992. Rapid solutions of problems by quantum computation. *Proceedings of the Royal Society of London* 439, 1907, 553–558.

Ma Ding and Fan Jing. 2010. Digital image encryption algorithm based on improved Arnold transform. In *Proceedings of the IEEE International Forum on Information Technology and Applications (IFITA'10)*. 174–176.

P. A. M. Dirac. 1930. *Principles of Quantum Mechanics*. Oxford University Press.

Rashmi Dubey, Rajesh Prasad Singh, Sarika Jain, and Rakesh Singh Jadon. 2014. Quantum methodology for edge detection: A compelling approach to enhance edge detection in digital image processing. In *Proceedings of the 5th IEEE International Conference on Confluence: The Next Generation Information Technology Summit*. 631–636.

A. Einstein. 1965. Concerning an heuristic point of view toward the emission and transformation of light. *Annals of Physics* 33, 5.

Artur K. Ekert. 1991. Quantum cryptography based on Bell's theorem. *Physical Review Letters* 67, 6, 661–663.

A. Fijany and C. Williams. 1998. Quantum wavelet transforms: Fast algorithms and complete circuits. In *Proceedings of the 1st NASA International Conference on Quantum Computing and Quantum Communications*. 10–33.

X.-W. Fu, M.-Y. Ding, and C. Cai. 2010. Despeckling of medical ultrasound images based on quantum-inspired adaptive threshold. *IET Electronics Letters* 24, 13, 889–891.

S. K. Ghosh. 2013. *Digital Image Processing.* Alpha Science International Ltd.

Nicolas Gisin. 2014. *Quantum Chance.* Copernicus.

Rafael C. Gonzalez and Richard E. Woods. 2007. *Digital Image Processing* (3rd ed.). Pearson.

Lov K. Grover. 1996. A fast quantum mechanical algorithm for database search. In *Proceedings of the 28th Annual ACM Symposium on the Theory of Computing*. 212–219.

Jozef Gruska. 1999. *Quantum Computing*. McGraw-Hill.

Shon Harris. 2012. Cryptography. In *CISSP All-in-One Exam Guide*. McGraw-Hill.

W. Heisenberg. 1927. Ueber den anschaulichen inhalt der quantentheoretischen kinematik und mechanik. *Zeitschrift Für Physik* 43, 172–198.

Anthony T. S. Ho, Jun Shen, Soon Hie Tan, and Alex C. Kot. 2002. Digital image-in-image watermarking for copyright protection of satellite images using the fast Hadamard transform. In *Proceedings of the IEEE International Geoscience and Remote Sensing Symposium (IGARSS'02)*. 3311–3313.

Mengyue Hu, Xiaolin Tian, Shaowei Xia, and Yue Qin. 2010. Image scrambling based on 3-D Hilbert curve. In *Proceedings of the 3rd IEEE International Congress on Image and Signal Processing (CISP'10)*. 147–149.

Tianxiang Hua, Jiamin Chen, Dongju Pei, Wenquan Zhang, and Nanrun Zhou. 2015. Quantum image encryption algorithm based on correlation decomposition. *International Journal of Theoretical Physics* 54, 2, 526–537.

Abdullah M. Iliyasu. 2013. Towards realising secure and efficient image and video processing applications on quantum computers. *MDPI Journal of Entropy* 15, 8, 2874–2974.

Abdullah M. Iliyasu, Phuc Q. Le, Fangyan Dong, and Kaoru Hirota. 2012. Watermarking and authentication of quantum images based on restricted geometric transformations. *Journal of Information Sciences* 186, 1, 126–149.

Abdullah M. Iliyasu, Phuc Q. Le, Fangyan Dong, and Kaoru Hirota. 2011. A framework for representing and producing movies on quantum computers. *International Journal of Quantum Information* 9, 6, 1459–1497.

Nan Jiang and Luo Wang. 2015. Quantum image scaling using nearest neighbor interpolation. *Springer Journal of Quantum Information Processing* 14, 5 (2015), 1559–1571.

Nan Jiang, Luo Wang, and Wen-Ya Wu. 2014a. Quantum Hilbert image scrambling. *International Journal of Theoretical Physics* 53, 7, 2463–2484.

Nan Jiang, Wen-Ya Wu, and Luo Wang. 2014b. The quantum realization of Arnold and Fibonacci image scrambling. *Springer Journal of Quantum Information Processing* 13, 5 (2014), 1223–1236.

Nan Jiang, Wen-Ya Wu, Luo Wang, and Na Zhao. 2015. Quantum image pseudocolor coding based on the density-stratified method. *Quantum Information Processing* 14, 5, 1735–1755.

Mamta Juneja and Parvinder Singh Sandhu. 2009. Performance evaluation of edge detection techniques for images in spatial domain. *International Journal of Computer Theory and Engineering* 1, 5, 614–621.

James Kakalios. 2011. *The Amazing Story of Quantum Mechanics: A Math-Free Exploration of the Science That Made Our World*. Avery.

Akshay K. Kallianpur, M. V. Bharath, and K. Manikantan. 2015. Digital image watermarking using optimized transform-domain approach. In *Proceedings of the IEEE UP Section Conference on Electrical Computer and Electronics (UPCON'15)*. 1–6.

S. K. Katiyar and P. V. Arun. 2014. Comparative analysis of common edge detection techniques in context of object extraction. *IEEE Transactions on Geoscience and Remote Sensing* 50, 11, 68–79.

Akhil Kaushik, Krishan Gupta, and Anant Kumar. 2014. Digital image chaotic encryption (DICE—a partial-symmetric key cipher for digital images). In *Proceedings of the IEEE International Conference on Reliability, Optimization, and Information Technology*. 314–317.

Vivien Kendon and William Munro. 2006. Entanglement and its role in Shor's algorithm. *Quantum Information and Computation* 6, 7, 630–640.

Faisal Shah Khan. 2009. *Doctoral Dissertation: Quantum Multiplexers, Parrondo Games, and Proper Qunatization*. Ph.D. Dissertation. Portland State University, Portland, OR.

Andreas Klappenecker and Martin Rotteler. 2001. Discrete cosine transforms on quantum computers. In *Proceedings of the 2nd IEEE International Symposium on Image and Signal Processing and Analysis (ISPA'01)*. 464–468.

Marco Lanzagorta and Jeffrey Uhlmann. 2008. *Quantum Computer Science*. Synthesis Lectures on Quantum Computing Series. Morgan & Claypool.

Jose I. Latorre. 2005. Image compression and entanglement. arXiv:0510031.

Phuc Q. Le, Fangyan Dong, and Kaoru Hirota. 2010. A flexible representation of quantum images for polynomial preparation, image compression, and processing operations. *Quantum Information Processing* 10, 1, 63–84.

Phuc Q. Le, Abdullah M. Iliyasu, Fangyan Dong, and Kaoru Hirota. 2011a. Efficient color transformations on quantum images. *Journal of Advanced Computational Intelligence and Intelligent Informatics* 15, 6, 698–706.

Phuc Q. Le, Abdullahi M. Iliyasu, Fangyan Dong, and Kaoru Hirota. 2011b. A flexible representation and invertible transformations for images on quantum computers. In *New Advances in Intelligent Signal Processing*. Studies in Computational Intelligence, Vol. 372. Springer, 179–202.

Phuc Q. Le, Abdullahi M. Iliyasu, Fangyan Dong, and Kaoru Hirota. 2011c. Strategies for designing geometric transformations on quantum images. *Theoretical Computer Science* 412, 15, 1406–1418.

Phuc Q. Le, Abdullahi M. Iliyasu, Fangyan Dong, and Kaoru Hirota. 2010. Fast geometric transformations on quantum images. *International Journal of Applied Mathematics* 40, 3, 1–11.

Hai-Sheng Li, Qingxin Zhu, Rigui Zhou, Yonghua Pu, and Lan Song. 2014. Image storage, retrieval and compression in entangled quantum systems. In *Proceedings of the IEEE International Conference on Progress in Informatics and Computing (PIC'14)*. 237–241.

Hai-Sheng Li, Zhu Qingxin, Song Lan, Chen-Yi Shen, Rigui Zhou, and Jia Mo. 2013a. Image storage, retrieval, compression and segmentation in a quantum system. *Quantum Information Processing* 12, 6, 2269–2290.

Hai-Sheng Li, Qingxin Zhu, Ri-Gui Zhou, Lan Song, and Xing-Jiang Yang. 2013b. Multi-dimensional color image storage and retrieval for a normal arbitrary quantum superposition state. *Quantum Information Processing* 13, 4, 991–1011.

Rui Lie and Xiao Ping Tian. 2011. A space-bit-plane scrambling algorithm for image based on chaos. *Journal of Multimedia* 6, 5, 458–466.

Seth Lloyd, Silvano Garnerone, and Paolo Zanardi. 2016. Quantum algorithms for topological and geometric analysis of data. *Nature Communications* 7, 10138.

Chris Lomont. 2003. Quantum convolution and quantum correlation algorithms are physically impossible. arXiv:quant-ph/0309070.

J. P. Maheshwari, M. Kumar, G. Mathur, R. P. Yadav, and R. Kumar Kakerda. 2015. Robust digital image watermarking using DCT based pyramid transform via image compression. In *Proceedings of the IEEE International Conference on Communications and Signal Processing (ICCSP'15)*. 1059–1063.

Mario Mastriani. 2014a. Quantum Boolean image denoising. *Quantum Information Processing* 14, 5, 1573–1332.

Mario Mastriani. 2014b. Quantum edge detection for image segmentation in optical environments. arXiv:1409.2918.

Mario Mastriani. 2016. Quantum image processing? arXiv:1512.02942.

Nathaniel David Mermin. 2007. *Quantum Computer Science: An Introduction*. Cambridge University Press.

S. Meshoul and A. Al Hussaini. 2009. Image processing using quantum computing and reverse emergence. *International Journal of Nano and Biomaterials* 2, 6, 136–142.

M. Mishra, P. Mishra, M. C. Adhikary, and S. Kumar. 2012. Image encryption using Fibonacci-Lucas transformation. *International Journal on Cryptography and Information Security* 2, 3, 131–141.

Gordon E. Moore. 1965. Cramming more components onto integrated circuits. *Proceedings of the IEEE* 86, 1, 82–85.

Hossein Nezamabadi-Pour, Saeid Saryazdi, and Esmat Rashedi. 2006. Edge detection using ant algorithms. *Soft Computing* 10, 7, 623–628.

Michael A. Nielsen and Isaac L. Chuang. 2000. *Quantum Computation and Quantum Information.* Cambridge University Press.

Jingfeng Pan, Tieyong Cao, Xiong Wei Zhang, and Hui Huang. 2012. A quantum-inspired noise reduction method based on noise feature codebook. In *Proceedings of the IEEE International Conference on Computer Vision in Remote Sensing (CVRS'12)*. 158–163.

J. M. Parmar and S. A. Patil. 2013. Performance evaluation and comparison of modified denoising method and the local adaptive wavelet image denoising method. In *Proceedings of the IEEE International Conference on Intelligent Systems and Signal Processing (ISSP'13)*. 101–105.

Pawan Patidar, Manoj Gupta, Sumit Srivastava, and Ashok Kumar Nagawat. 2010. Image de-noising by various filters for different noise. *International Journal of Computer Applications* 9, 4, 45–50.

Pietro Perona and Jitendra Malik. 1990. Scale-space and edge detection using anisotropic diffusion. *IEEE Transactions on Pattern Analysis and Machine Intelligence* 12, 7, 629–639.

Vidyasagar M. Potdar, Song Han, and Elizabeth Chang. 2005. A survey of digital image watermarking techniques. In *Proceedings of the IEEE International Conference on Industrial Informatics (INDIN'05)*. 709–716.

Yang Qianli and Cai Yanhong. 2012. A digital image watermarking algorithm based on discrete wavelet transform and discrete cosine transform. In *Proceedings of the IEEE International Symposium on Information Technology in Medicine and Education (ITME'12)*. 1102–1105.

Phuc Le Quang, Fangyan Dong, Yoshinori Arai, and Kaoru Hirota. 2009. Flexible representation of quantum images and its computational complexity analysis. In *Proceedings of the Fuzzy System Symposium.* 185–185.

Abhijeet A. Ravankar and Stanislav G. Sedukhin. 2011. Image scrambling based on a new linear transform. In *Proceedings of the IEEE International Conference on Multimedia Technology (ICMT'11)*. 3105–3108.

Philippe Refregier and Bahram Javidi. 1995. Optical image encryption based on input plane and Fourier plane random encoding. *International Journal of Theoretical Physics* 20, 7, 767–769.

David J. Reilly. 2015. Engineering the quantum-classical interface of solid-state qubits. *NPJ Quantum Information* 1, 6, Article No. 15011.

Eleanor Rieffel and Wolfgang Polak. 2000. An introduction to quantum computing for non-physicists. *ACM Computing Surveys* 32, 2, 300–335.

K. F. Riley, M. P. Hobson, and S. J. Bence. 2006. *Mathematical Methods for Physics and Engineering* (3rd ed.). Cambridge University Press.

Ahmed Salama, Randa Atta, Rawya Rizk, and Fayez Wanes. 2011. A robust digital image watermarking technique based on wavelet transform. In *Proceedings of the IEEE International Conference on System Engineering and Technology (ICSET'11)*. 100–105.

Erwin Schrödinger. 1926. An undulatory theory of the mechanics of atoms and molecules. *Physical Review* 28, 6.

N. Senthilkumaran and R. Rajesh. 2009. Edge detection techniques for image segmentation a survey of soft computing approaches. *International Journal of Recent Trends in Engineering* 1, 2, 250–254.

Peter Shor. 1997. Polynomial-time algorithms for prime factorization and discrete logarithms on a quantum computer. *SIAM Journal on Computing* 26, 5, 1484–1509.

Mona M. Soliman, Aboul Ella Hassanien, and Hoda M. Onsi. 2015. An adaptive watermarking approach based on weighted quantum particle swarm optimization. *Neural Computing and Applications* 27, 2, 469–481.

Xian-Hua Song, Shen Wang, Ahmed A. Abd El-Latif, and Xiamu Niu. 2014a. Dynamic watermarking scheme for quantum images based on Hadamard transform. *Multimedia Systems* 20, 4, 379–388.

Xian-Hua Song, Shen Wang, Ahmed A. Abd El-Latif, and Xia-Mu Niu. 2014b. Quantum image encryption based on restricted geometric and color transformations. *Quantum Information Processing* 13, 8, 1765–1787.

Xian-Hua Song, Shen Wang, Shuai Liu, Ahmed A. Abd El-Latif, and Xia-Mu Niu. 2013. A dynamic watermarking scheme for quantum images using quantum wavelet transform. *Quantum Information Processing* 12, 12, 3689–3706.

Xian-Hua Song, Shen Wang, and Xia-Mu Niu. 2013. Multi-channel quantum image representation based on phase transform and elementary transformations. *Information Hiding and Multimedia Signal Processing* 5, 4, 574–585.

Milan Sonka, Vaclav Hlavac, and Roger Boyle. 1993. *Image Processing, Analysis, and Machine Vision* (3rd ed.). Springer.

T. Sridevi and S. Sameen Fatima. 2013. Digital image watermarking using genetic algorithm in DWT and SVD transform. In *Proceedings of the IEEE 3rd International Conference on Computational Intelligence and Information Technology (CIIT'13)*. 485–490.

Bo Sun, Abullah M. Iliyasu, Fei Yan, and Kaoru Hirota. 2013a. An RGB multi-channel representation for images on quantum computers. *Journal of Advanced Computational Intelligence and Intelligent Informatics* 17, 3, 404–417.

Bo Sun, Phuc Q. Le, Abullah M. Iliyasu, Fei Yan, J. Adrian Garcia, Fangyan Dong, and Kaoru Hirota. 2013b. A two-tier scheme for greyscale quantum image watermarking and recovery. *International Journal of Innovative Computing and Applications* 5, 2, 85–101.

Bo Sun, Phuc Q. Le, Abdullah M. Iliyasu, Fei Yan, Jesus A. Garcia, Fangyan Dong, and Kaoru Hirota. 2011. A multi-channel representation for images on quantum computers using RGBα color space. In *Proceedings of the IEEE International Symposium on Intelligent Signal Processing (WISP'11)*. 1–6.

Jun Sun, Bin Feng, and Wenbo Xu. 2004. Particle swarm optimization with particles having quantum behavior. In *Proceedings of the IEEE Congress on Evolutionary Computation*. 325–331.

Leonard Susskind. 2015. *Quantum Mechanics: The Theoretical Minimum*. Basic Books.

Hichem Talbi, Mohamed Batouche, and Amer Draa. 2007. A quantum-inspired evolutionary algorithm for multiobjective image segmentation. *International Journal of Mathematical, Physical and Engineering Sciences* 1, 2, 109–114.

Gu Tianming and Wang Yanjie. 2011. DWT-based digital image watermarking algorithm. In *Proceedings of the IEEE International Conference on Electronic Measurement and Instruments (ICEMI'11)*. 163–166.

Carlo Tomasi and Roberto Manduchi. 1998. Bilateral filtering for gray and color images. In *Proceedings of the IEEE International Conference on Computer Vision (ICCV'98)*. 839–846.

Salvador E. Venegas-Andraca. 2015. Introductory words: Special issue on quantum image processing. *Quantum Information Processing* 14, 5, 1535–1537.

S. E. Venegas-Andraca and J. L. Ball. 2010. Processing images in entangled quantum systems. *Quantum Information Processing* 9, 1, 1–11.

Salvador E. Venegas-Andraca and Sougato Bose. 2003a. Quantum computation and image processing: New trends in artificial intelligence. In *Proceedings of the International Conference on Artificial Intelligence.* 1563–1564.

Salvador E. Venegas-Andraca and Sougato Bose. 2003b. Storing, processing, and retrieving an image using quantum mechanics. *SPIE Proceedings on Quantum Information and Computation* 5105, 137–147.

Rohit Verma and Jahid Ali. 2013. A comparative study of various types of image noise and efficient noise removal techniques. *International Journal of Advanced Research in Computer Science and Software Engineering* 3, 10, 617–622.

Alexander Yu. Vlasov. 1997. Quantum computations and image recognition. arXiv:quant-ph/9703010.

Jian Wang, Nan Jiang, and Luo Wang. 2015a. Quantum image translation. *Quantum Information Processing* 14, 5, 1589–1604.

Peng Wang and Jian-Ping Li. 2007. Wavelet denoising by quantum threshold algorithm. In *Proceedings of the 4th IEEE International Conference on Image and Graphics*. 62–66.

Qiang Wang, Qun Ding, Zhong Zhang, and Lina Ding. 2008. Digital image encryption research based on DWT and chaos. In *Proceedings of the 4th IEEE International Conference on Natural Computation*. 494–498.

Shen Wang, Xianhua Song, and Xiamu Niu. 2014. A novel encryption algorithm for quantum images based on quantum wavelet transform and diffusion. In *Intelligent Data Analysis and Its Applications*. Advances in Intelligent Systems and Computing, Vol. 298. Springer, 243–250.

Z. Wang and B. Hunt. 1983. The discrete cosine transform—a new version. In *Proceedings of the IEEE International Conference on Acoustics, Speech, and Signal Processing (ICASSP'83)*, Vol. 8. 1256–1259.

Shen Wang, Jianzhi Sang, Xianhua Song, and Xiamu Niu. 2015b. Least significant qubit (LSQb) information hiding algorithm for quantum image. *Journal of Measurement* 73, 352–359.

Fei Yan, Abdullah M. Iliyasu, Chastine Fatichah, Martin L. Tangel, Janet P. Betancourt, Fangyan Dong, and Kaoru Hirota. 2012a. Quantum image searching based on probability distributions. *Journal of Quantum Information Science* 2, 55–60.

Fei Yan, Abdullah M. Iliyasu, and Zhengang Jiang. 2014. Quantum computation-based image representation, processing operations and their applications. *MDPI Journal of Entropy* 16, 10, 5290–5338.

Fei Yan, Abdullah M. Iliyasu, and Salvador E. Venegas-Andraca. 2016. A survey of quantum image representations. *Quantum Information Processing* 15, 1, 1–35.

Fei Yan, Abdullah M. Iliyasu, Salvador E. Venegas-Andraca, and Huamin Yang. 2015b. Video encryption and decryption on quantum computers. *International Journal of Theoretical Physics* 54, 8, 2893–2904.

Fei Yan, Phuc Q. Le, Abdullah M. Iliyasu, Bo Sun, Jesus A. Garcia, Fangyan Dong, and Kaoru Hirota. 2012b. Assessing the similarity of quantum images based on probability measurements. In *Proceedings of the Congress on Evolutionary Computation*. 1–6.

Yu-Guang Yang, Xin Jia, Si-Jia Sun, and Qing-Xiang Pan. 2014. Quantum cryptographic algorithm for color images using quantum Fourier transform and double random-phase encoding. *Information Sciences* 277, 445–457.

Yu-Guang Yang, Xin Jia, Peng Xu, and Ju Tian. 2013a. Analysis and improvement of the watermark strategy for quantum images based on quantum Fourier transform. *Quantum Information Processing* 12, 8, 2765–2769.

Yu-Guang Yang, Juan Xia, Xin Jia, and Hua Zhang. 2013b. Novel image encryption/decryption based on quantum Fourier transform and double phase encoding. *Quantum Information Processing* 12, 11, 3477–3493.

Yu-Guang Yang, Peng Xu, Ju Tian, and Hua Zhang. 2014. Analysis and improvement of the dynamic watermarking scheme for quantum images using quantum wavelet transform. *Quantum Information Processing* 13, 9, 1931–1936.

Zhang Yi, Lu Kai, and Gao YingHui. 2014. Sobel: A novel quantum image edge extraction algorithm. *Science China Information Sciences* 24, 1, 1–13.

Akram Youssry, Ahmed El-Rafei, and Salwa Elramly. 2015. A quantum mechanics-based framework for image processing and its application to image segmentation. *Quantum Information Processing* 14, 10, 3613–3638.

Suzhen Yuan, Xia Mao, Tian Li, Yuli Xue, Lijiang Chen, and Qingxu Xiong. 2014a. Quantum morphology operations based on quantum representation model. *Quantum Information Processing* 14, 5, 1625–1645.

Suzhen Yuan, Xia Mao, Yuli Xue, Lijiang Chen, Qingxu Xiong, and Angelo Compare. 2014b. SQR: A simple quantum representation of infrared images. *Quantum Information Processing* 13, 6, 1353–1379.

Suzhen Yuan, Xia Maoa, Lijiang Chena, and Yuli Xueaa. 2013. Quantum digital image processing algorithms based on quantum measurement. *Journal of Optik* 124, 23, 6386–6390.

Yusnita Yusof and Othman O. Khalifa. 2007. Digital watermarking for digital images using wavelet transform. In *Proceedings of the IEEE International Conference on Telecommunications and Malaysia International Conference on Communications*. 665–669.

Jian Zhang, Jiliu Zhou, Kun He, and Huanzhou Li. 2012. Image edge detection using quantum ant colony optimization. *International Journal of Digital Content Technology and Its Applications* 6, 11, 187–195.

Qi Zhang and Qun Ding. 2015. Digital image encryption based on advanced encryption standard (AES). In *Proceedings of the 5th IEEE International Conference on Instrumentation and Measurement, Computer, Communication, and Control (IMCCC'15)*. 1218–1221.

Wei-Wei Zhang, Fei Gao, Bin Liu, Heng-Yue Jia, Qiao-Yan Wen, and Hui Chen. 2013a. A quantum watermark protocol. *International Journal of Theoretical Physics* 52, 2, 504–513.

Wei-Wei Zhang, Fei Gao, Bin Liu, Qiao-Yan Wen, and Hui Chen. 2013b. A watermark strategy for quantum images based on quantum Fourier transform. *Quantum Information Processing* 12, 2, 793–803.

Yi Zhang, Kai Lu, Yinghui Gao, and Mo Wang. 2013c. NEQR: A novel enhanced quantum representation of digital images. *Quantum Information Processing* 12, 8, 2833–2860.

Yi Zhang, Kai Lu, Yinghui Gao, and Kai Xu. 2013d. A novel quantum representation for log-polar images. *Quantum Information Processing* 12, 9, 3103–3126.

Yi Zhang, Kai Lu, Kai Xu, Yinghui Gao, and Richard Wilson. 2015. Local feature point extraction for quantum images. *Quantum Information Processing* 14, 5, 1573–1588.

Changxiong Zhou, Zhifeng Hu, Feng Wang, Haijiang Fan, and Li Shang. 2010. Quantum collapsing median filter. In *Advanced Intelligent Computing Theories and Applications*. Communications in Computer and Information Science, Vol. 93. 454–461.

Ri-Gui Zhou, Zhi Bo Chang, Ping Fan, Wei Li, and Tian Tian Huan. 2015b. Quantum image morphology processing based on quantum set operation. *International Journal of Theoretical Physics* 54, 6, 1974–1986.

Ri-Gui Zhou and Ya-Juan Sun. 2015. Quantum multidimensional color images similarity comparison. *Quantum Information Processing* 14, 5, 1605–1624.

Ri-Gui Zhou, Ya-Juan Sun, and Ping Fan. 2015c. Quantum image gray-code and bit-plane scrambling. *Quantum Information Processing* 14, 5, 1717–1734.

Ri-Gui Zhou, Qian Wu, Man-Qun Zhang, and Chen-Yi Shen. 2012. Quantum image encryption and decryption algorithms based on quantum image geometric transformations. *International Journal of Theoretical Physics* 52, 6, 1802–1817.

Xiao Zhou, Yunhao Bai, and Chengyou Wang. 2015a. Image compression based on discrete cosine transform and multistage vector quantization. *International Journal of Multimedia and Ubiquitous Engineering* 10, 6, 347–356.

Guiliang Zhu, Weiping Wang, Xiaoqiang Zhang, and Mengmeng Wang. 2010. Digital image encryption algorithm based on pixels. In *Proceedings of the IEEE International Forum on Information Technology and Applications*. 769–772.

Jiancheng Zou and Rabab K. Ward. 2003. Introducing two new image scrambling methods. In *Proceedings of the IEEE Pacific Rim Conference on Communications, Computers, and Signal Processing*. 708–711.

Received July 2015; revised September 2016; accepted October 2016